UNIVERSITY OF COPENHAGEN
FACULTY OF SCIENCE

Masters thesis

Phillip Mercebach

Disorder in Topological Superconducting Wires

Advisor: Karsten Flensberg

Handed in: May 20, 2021

Disorder in Topological Superconducting Wires

Phillip Mercebach*

May 20, 2021

Abstract

This thesis sets out to investigate the effects of magnetic and non-magnetic disorder in superconducting systems. Of particular interest are topological superconducting wires and how impurity disorder in the lattice can effect such systems. We extend the BCS theory of superconductivity and use the self-consistent Born approximation to create a low correlation and weak density disorder model to predict the influence of impurities. The formalism developed is able to take into account low fillings of the superconductor. In bulk s-wave superconductivity we find results in accordance with Anderson's theorem contrasted to magnetic impurities which affect the density of states. Our main result is for bulk p-wave superconductivity where we find both magnetic and non-magnetic type disorder affect the model equally. Finally we use these results to infer the effect of disorder in 1D wire systems on Majorana edge modes.

*Phillip(.)mercebach@gmail.com

Contents

1 Introduction

The topic of this thesis is to investigate the effects of disorder in superconducting materials. We do this by analyzing the tunneling density of states. Of particular interest and focus is the one dimensional topological superconducting wire. Many of the results are derived using a self-consistent implementation of the first Born approximation scheme. These approximation methods can be explained using diagrammatics within the Green's function formalism of single (quasi-) particle interactions. That is, we are working from a standpoint of assumed low correlations and low disorder density which we discuss the justification of in detail.

The underlying motivation for this thesis stems from proximity induced superconductivity in a semiconductor with spin-orbit interaction subject to a strong magnetic field giving rise to topological superconductivity. In such a proximitized system the existence of Majorana modes has been proposed near the ends of the wire. Such Majorana modes exhibit stability from decoherence because of their non-local natureand and may be useful for realizing qubits and quantum computers. It is of interest to those producing such systems what kind of margins there is in the manufacturing process with regards to disorder and impurities. So we seek out to investigate what happens when impurities are added to otherwise ideal superconducting systems.

The thesis is given a chronological structure, the preliminaries for both theory and experimental notions are detailed in this introductory chapter. Then it moves on to give a brief introduction to the Green's function formalism and BCS theory of superconductivity. One of our main results will be to reproduce and generalize results from long standing methods such as covered in Rickayzen [10]. These results are compared and contrasted with my own exact analytical calculations in Chapter 2.2.

We shall introduce a model used for topological superconductivity in 1D similar to the presentation given in Oreg et. al. [9]. This model is a modified BCS model including both spin-orbit interactions and an externally supplied magnetic field. We use a Schriefer Wolff approximation to find this equivalent to a p-wave superconducting model and apply the Born approximation. The results are compared extensively to the BCS formalism in Chapter 2.5.

Moving on to the preliminaries. Let's start by introducing the important *second quantization*, I shall do this rather physically and not care about the specifics of deriving the algebra mathematically. In quantum mechanics the motion of particles are described by *Schrödinger's equation*

$$H\psi(x) = E\psi(x) \tag{1.1}$$

where H is the *energy operator*, called the *Hamiltonian*, E is the energy of the particle and ψ is the wave function such that $|\psi|^2$ is the probability distribution in space (and time), i.e. the likelyhood of where the particle can be observed. Another way of writing the wave function ψ is to use *bra-ket notation* so that the ket $|\psi\rangle$ represents the wave function in Schrödinger's equation above. The advantage of this notation comes when the system in consideration may effectively be described by *quantum numbers* such as momentum k or spin $\sigma = \uparrow, \downarrow$. This simply means all all the relevant information of the system may be described using these quantum numbers and how they relate to Schrödinger's equation. Then we write the wavefunction as $|k, \sigma\rangle$ for a particle with momentum k and spin σ–which can be either up or down in this case. As an abstraction we may collect such quantum numbers in a single symbol like ν, e.g. $|\nu\rangle$ meaning a particle in a state described with quantum number(s) ν.

Now, for many particle systems it is convenient to introduce the *occupation number representation* where we write $|n_{\nu_1}, n_{\nu_2}, \ldots\rangle$ for a system with n_{ν_1} particles described by the quantum number ν_1 and n_{ν_2} in state ν_2 and so on. We can change the number of particles by inserting or removing a particle in state ν_i by writing either $|\ldots, n_{\nu_i} + 1, \ldots\rangle$ or $|\ldots, n_{\nu_i} - 1, \ldots\rangle$. To do this formally we define so called *creation* and *annihilation* operators $\psi^\dagger_{\nu_i}$ and ψ_{ν_i}, respectively. They are simply functions acting on the wave function kets either creating or removing a particle from the system. In detail they either create or remove a particle in the state ν_i from the system, respectively, e.g.

$$\psi^\dagger_{\nu_i} |\ldots, n_{\nu_i}, \ldots\rangle \propto |\ldots, n_{\nu_i} + 1, \ldots\rangle \quad \text{and} \quad \psi_{\nu_i} |\ldots, n_{\nu_i}, \ldots\rangle \propto |\ldots, n_{\nu_i} - 1, \ldots\rangle \tag{1.2}$$

These creation and annihilation operators create a basis for making all possible combinations of many body particle configurations so any Hamiltonian may be expressed in terms of these, e.g. the free particle kinetic energy operator takes the form

$$T = \sum_k \psi^\dagger_k \frac{\hbar^2 k^2}{2m} \psi_k. \tag{1.3}$$

We call T the second quantized form of the kinetic energy operator. Notice the 'first quantized', or at least the more familiar form, is sandwiched between the second quantized operators, namely the kinetic operator $\mathcal{T} = \frac{\hbar^2 k^2}{2m}$.

One particular idea which shall become very useful for our understanding of these exotic '1D' systems is the idea of quasi dimensionality and localization. Consider a free electron gas, i.e. non-interacting electrons, in some 2 dimensional material, e.g. a metallic conductor. If we add a strong constant potential V everywhere except a thin strip of width L along the x-axis we have then localized the electrons to this strip. But what does this mean, exactly? Although the electrons may still move as free particles along the x-direction, they have been confined to a square box in the y-direction occupying energy levels that are inversely proportional to L^2:

$$E_{n_y} = \frac{2\pi^2\hbar^2}{mL^2} n_y^2, \tag{1.4}$$

here n_y is the wave number in the y-direction. As the width of this strip L gets increasingly small the energy levels get proportionally more and more spaced out. So for very small widths L the higher energy levels, e.g. $n_y = 2$, are inaccessible to the electrons. So the electrons are forced to move along a long wire embedded in the 2 dimensional plane, effectively creating a 1D free electron gas.

There are many ways to realize such 1D systems. One of them is to selectively dope materials to increase or decrease the local potentials thus traping free electrons in such embedded wire structures. This is heavily utilized in the semiconductor industry. But in fact one can imagine an 2D insulating system and one may deposit or etch a metallic material on top in a pattern resembling two rectangles, of a distance apart L, covering a closed area of the insulator substrate. One can apply a voltage to these metallic gates and create the potential V in this fashion. This is particularly useful for tuning the filling of electrons in the conductance band of semiconductors

1.1 Superconductivity and its Microscopics

Electrical resistance can be explained as the obstruction of free electrons flowing in a material: as electrons move they may encounter atoms which introduces an electrical resistance. Superconductivity was fist discovered in 1911 by Heike K. Onnes who measured a zero resistivity of solid Mercury at temperatures below 4.2K. This temperature transition between a normal material and the superconducting state is called the *critical temperature*, T_c. Although there was many interesting experiments involving superconductors in the following years uncovering a manifold of exotic physics, see e.g. *the Meissner effect* or *Flux pinning*, the mechanism behind superconductivity explained until 1957. The explanation, provided by Berdeen, Cooper and Schrieffer [BCS] cemented the foundation for the modern study of superconductivity and in particular this thesis. Superconductivity may naively be defined as the absence of electrical resistance but in modern times the superconducting state is often defined as a perfect diamagnet as they expel magnetic fields perfectly.

Colloquially the BCS theory proposes an instability of the normal state system when cooled below a certain *critical temperature* T_c if the interactions between electrons becomes attractive. Through tedious and very careful calculations one can find by including the interactions of the lattice vibrations and the electrons the effective electron-electron interaction becomes attractive at certain energy levels below the critical temperature[1]. This causes pairs of electrons to *condense* into so called *Cooper pairs*. The Cooper pairs condensate move nigh unhindered in the material giving rise to superconductivity.

An informative picture to have in mind when thinking of this process is to consider an electron moving through the material, as it does it attracts, although only slightly, nearby atoms moving them closer, increasing the positive charge density locally. Any other nearby electron will be attracted to this locally positive charge forming the cooper pair. Throughout the whole lattice many such pairs are created forming a so called condensate.

Mathematically we can describe this model through the Hamiltonian of a free electron gas with an attractive electron-electron interaction potential between $V_{\mathbf{k},\mathbf{k}'}$ as follows

$$H_{\text{BCS}} = \sum_{\mathbf{k},\sigma} \xi_{\mathbf{k}} \psi^\dagger_{\mathbf{k}\sigma} \psi_{\mathbf{k}\sigma} + \sum_{\mathbf{k}\mathbf{k}'} V_{\mathbf{k},\mathbf{k}'} \psi^\dagger_{\mathbf{k}\uparrow} \psi^\dagger_{-\mathbf{k}\downarrow} \psi_{-\mathbf{k}'\downarrow} \psi_{\mathbf{k}'\uparrow}, \tag{1.5}$$

where $V_{\mathbf{k},\mathbf{k}'} < 0$ for energies lower than the Debye frequency and $\xi_{\mathbf{k}} = \mathbf{k}^2/2m - \mu$ is the electron spectrum with chemical potential μ. By doing a Hartree Fock Mean Field approximation, see Appendix C for details, we obtain the familiar BCS mean-field Hamiltonian

$$H^{\text{MF}}_{\text{BCS}} = \sum_{\mathbf{k},\sigma} \xi_{\mathbf{k}} \psi^\dagger_{\mathbf{k}\sigma} \psi_{\mathbf{k}\sigma} + \sum_{\mathbf{k}} [\Delta_{\mathbf{k}} \psi^\dagger_{\mathbf{k}\uparrow} \psi^\dagger_{-\mathbf{k}\downarrow} + h.c.] \quad \text{where} \quad \Delta_{\mathbf{k}} := \sum_{\mathbf{k}'} V_{\mathbf{k},\mathbf{k}'} \langle \psi_{\mathbf{k}'\downarrow} \psi_{-\mathbf{k}'\uparrow} \rangle . \tag{1.6}$$

Here "h.c." denotes the Hermitian conjugate of the previous term and $\langle - \rangle$ is the thermal average.

[1] Note there may be another mechanism behind generating an attractive effective electron-electron interaction than lattice vibrations, see for example the mechanisms behind different types of unconventional superconductivity. But it is generally accepted that whatever mechanism is behind this attractive potential, once there, it allows for superconductivity.

Because of the structure of this Hamiltonian we are able to describe it more simply using the so called *Nambu Spinors*, in imaginary time τ

$$\Psi^\dagger_{\mathbf{k}}(\tau) := \begin{pmatrix} \psi^\dagger_{\mathbf{k}\uparrow}(\tau) & \psi_{-\mathbf{k}\downarrow}(\tau) \end{pmatrix} \quad \text{and} \quad \Psi_{\mathbf{k}}(\tau) := \begin{pmatrix} \psi_{\mathbf{k}\uparrow}(\tau) \\ \psi^\dagger_{-\mathbf{k}\downarrow}(\tau) \end{pmatrix}. \tag{1.7}$$

This enables the definition of the *Bogoliubov de Gennes* [BdG] Hamiltonian is as

$$\mathcal{H}^{\text{BdG}}_{\mathbf{k}} := \begin{pmatrix} \xi_{\mathbf{k}} & \Delta_{\mathbf{k}} \\ \Delta^*_{\mathbf{k}} & -\xi_{\mathbf{k}} \end{pmatrix}. \tag{1.8}$$

Such that the relation between the BCS mean field Hamiltonian and the BdG is $H^{\text{MF}}_{\text{BCS}} = \sum_{\mathbf{k}} \Psi^\dagger_{\mathbf{k}} \mathcal{H}^{\text{BdG}}_{\mathbf{k}} \Psi_{\mathbf{k}}$. The eigenenergies of this BdG Hamiltonian are exactly the same as the BCS mean field Hamiltonian and are found to be $E_{\mathbf{k}\pm} = \pm\sqrt{\xi^2_{\mathbf{k}} + \Delta^2_{\mathbf{k}}}$, that is the gap function $\Delta_{\mathbf{k}}$ induces a gap in the spectrum of the system.

The BdG Hamiltonian has all the important characteristic information of the system. Conveniently we may write it in terms of the Pauli matrices, σ_i, as they contrive a basis for the 2×2 Hermitian matrices, as $\mathcal{H}^{\text{BdG}}_{\mathbf{k}} = \xi_{\mathbf{k}}\sigma_3 + \Delta_{\mathbf{k}}\sigma_+ + \Delta^*_{\mathbf{k}}\sigma_-$ where $\sigma_\pm = \frac{\sigma_1 \pm i\sigma_2}{2}$ and

$$\sigma_0 = \begin{pmatrix} 1 & 0 \\ 0 & 1 \end{pmatrix}, \quad \sigma_1 = \begin{pmatrix} 0 & 1 \\ 1 & 0 \end{pmatrix}, \quad \sigma_2 = \begin{pmatrix} 0 & -i \\ i & 0 \end{pmatrix} \quad \text{and} \quad \sigma_3 = \begin{pmatrix} 1 & 0 \\ 0 & -1 \end{pmatrix}. \tag{1.9}$$

If the gap function is chosen to be real this simplifies even further to the form $\mathcal{H}^{\text{BdG}}_{\mathbf{k}} = \xi_{\mathbf{k}}\sigma_3 + \Delta_{\mathbf{k}}\sigma_1$. To find the new energies of the system it is simply a matter of finding the eigenvalues of the BdG Hamiltonian, they are $E^2_{\mathbf{k}} = \xi^2_{\mathbf{k}} + |\Delta_{\mathbf{k}}|^2$. But one might realistically ponder as to the distribution of particles at these energies. To answer this we must apply *the Green's Function formalism*, the (imaginary time) *Green's function* is defined as

$$\mathcal{G}(\mathbf{k}, \tau) := -\left\langle T_\tau \Psi_{\mathbf{k}}(\tau) \Psi^\dagger_{\mathbf{k}}(0) \right\rangle, \tag{1.10}$$

where $\mathcal{T}_\tau$ is the imaginary time ordering. From this it can be shown, using the equations of motion, that it must satisfy the Green's function equation

$$(\partial_\tau - \mathcal{H}^{\text{BdG}}_{\mathbf{k}})\mathcal{G}(\mathbf{k}, \tau) = 1. \tag{1.11}$$

This algebraic equations is easily solved in Matsubara frequency space, $i\omega_n$, that is a discrete Fourier transform of τ, $(i\omega_n - \mathcal{H}^{\text{BdG}}_{\mathbf{k}})\mathcal{G}(\mathbf{k}, i\omega_n) = 1$, the solution is the Green's function

$$\mathcal{G}(\mathbf{k}, i\omega_n) = \begin{pmatrix} i\omega_n - \xi_{\mathbf{k}} & -\Delta_{\mathbf{k}} \\ -\Delta^*_{\mathbf{k}} & i\omega_n + \xi_{\mathbf{k}} \end{pmatrix}^{-1} = -\frac{1}{\omega^2_n + \xi^2_{\mathbf{k}} + |\Delta_{\mathbf{k}}|^2} \begin{pmatrix} i\omega_n + \xi_{\mathbf{k}} & \Delta_{\mathbf{k}} \\ \Delta^*_{\mathbf{k}} & i\omega_n - \xi_{\mathbf{k}} \end{pmatrix}. \tag{1.12}$$

As we shall see below the Green's function contain much of the important information about the system. For example doing a Wick rotation ($i\omega_n \to \omega + i\eta$) and taking the imaginary part one can find the *density of states* of the system. Colloquially the density of states is the distribution of particles as a function of energies, i.e. at which energies are you more likely to find particles.

On a final note let's build some intuition of what this Green's Function is physically. From the defining equation, eq. (1.10), the Green's function is the expectation value of the time ordered field operators $\Psi_{\mathbf{k}}(\tau)\Psi^\dagger_{\mathbf{k}}(0)$. This pair of operators simply mean creating a particle at time 0 with momentum $\mathbf{k}$ and removing a particle at time τ with that same momentum. As an analogy we can think of a billiard table: the Green's function represents the probability of putting a ball on the table with momentum k and then at a later time τ taking out a ball with that same momentum. In this analogy the system is the billiard table with however many balls might be on it. After the billiard ball is inserted it can move around and disturb the system by hitting other billiard balls and thereby scattering into other momentum states.

1.2 Majorana Fermions, Tunneling Experiments and Quantum Computing

A large proportion of modern research in condensed matter physics has some kind of relation to quantum computing. There is a great ongoing discussion of how these quantum computers can be best realized physically depending on their specifications. In this chapter we introduce one proposed method involving the so called *Majorana Fermions* and consider how they can be used for quantum computing.

Majorana Fermions are a emergent phenomenon in condensed matter physics and appear near boundaries in their parent systems, e.g. a 1D wire geometry they might appear near the edge of the wire. We give a brief

introduction to these special particles based on Leijnse et. al. [7]. Consider a mathematical model of a wire system where the particles can 'hop' between different sites,

$$H_{\text{wire}} = \sum_{i=1}^{N-1} t c_i^\dagger c_{i+1} + \text{h.c.}, \tag{1.13}$$

where $c_i^\dagger$ and c_i create and remove a particle at site i. We can rewrite this model by defining canonical *Majorana operators* meaning they are Hermitian

$$\gamma_{i,1} := c_i^\dagger + c_i \quad \text{and} \quad \gamma_{i,2} := i(c_i^\dagger - c_i) \quad \text{such that} \quad c_i^\dagger = \frac{1}{2}(\gamma_{i,1} - i\gamma_{i,2}) \quad \text{and} \quad c_i = \frac{1}{2}(\gamma_{i,1} + i\gamma_{i,2}). \tag{1.14}$$

So far this is simply another way of expressing the same creation and annihilation operators at each site i, but we now have twice as many of them, $2N$ to be exact. Essentially we have a $2N$ lattice instead consisting of these γ operators, particularly we can relabel them into $\gamma_1, \ldots, \gamma_{2N}$. Combining these into $N-1$ non-locally paired operators $f_i := \frac{1}{2}(\gamma_{2i-1} + i\gamma_{2i})$ that consist of operators on neighbouring sites rather than the same site, we can rewrite the Hamiltonian as

$$H_{\text{wire}} = 2t \sum_{i=1}^{N-1} f_i^\dagger f_i. \tag{1.15}$$

Notice the ends $\gamma_{N,2}$ and $\gamma_{1,1}$ are left out from this expression! Combining the two Majorana operators at the end of the wire into the single Fermionic operator

$$f_M = \frac{1}{2}(\gamma_{2N} + i\gamma_1). \tag{1.16}$$

This is of course a highly non-local state comprised of the two local Majorana operators γ_1 and γ_{2N}. Since this *Majorana Fermion* is absent from the Hamiltonian the energy cost from occupying it is identically zero. This model is the most simple case where one can demonstrate Majorana physics. Importantly this same Majorana state can exist in a one dimensional p-wave superconductor.

But how are these Majorana edge modes used in quantum computation, surely we would need more than a single wire to make computation operations. By themselves they are not useful, but by arranging them in arrays, e.g. as proposed by Tutschku et. al. [13] or Karzig et. al. [6], one can by manipulating gate voltages *braid* the Majorana fermions. Braiding means rotating two Majorana modes around eachother and because of the non-abelian exchange statistics of these modes their wave function is changed in a non-trivial manner. This is exactly how the Majorana modes can be used as qubits and manipulated to realize quantum computation.

So how are these Majorana modes measured? Consider the following setup: A material is supplied with some voltage V and a metallic probe is brought close to the surface of the material. As a function of the voltage difference between the probe and the material V there is an induced current between the material and the probe that stems from electrons tunneling through the space between them. Mathematically one can show, see e.g. [3], the differential conductance is proportional to the spectral function A of the material at very low temperatures

$$\frac{\mathrm{d}I}{\mathrm{d}V} \propto \sum_{\mathbf{k}} A(\mathbf{k}, -eV), \tag{1.17}$$

where $-eV$ is the energy transfer of a single electron tunneling through the potential gap V. This spectral function is simply the imaginary part of the Green's function as defined in eq. (1.10)

$$A(\mathbf{k}, \omega) = -2\text{Im}[\mathcal{G}^R(\mathbf{k}, \omega + i\eta)]. \tag{1.18}$$

Particularly the spectral function is often called the (non-local) density of states [DOS]. As the Majorana mode is a zero energy excitation the indicator for the existence of a Majorana mode in a material is correlated to a peak at $\omega = 0$. Equivalently in the measurement setup described the Majorana mode occurs at $V = 0$ often called a *zero-bias peak* or ZBP for short.

Lastly let's mention the *proximity effect* which happens to materials in close proximity to a superconductor. In the interface between between a superconductor and a normal state (non-superconducting) material the cooper pairs can tunnel into the normal state material. This can induce superconductivity in the normal state material. The range of the induced superconductivity is limited by Cooper pairs scattering on impurities and other interactions in the normal state material causing decoherence in the tunneled Cooper pairs. Conversely the electrons of the normal state can tunnel into the superconductor through negatively affecting the superconducting state near the boundary. The proximity effect is a key component to realizing topological superconductors such as the 1D wire discussed above.

2 The Effects of Impurities in Bulk Superconductors

In this chapter we analyze the effects of impurities in superconductors. Particularly we follow the approach of Rickayzen [10] using a self-consistent method based on the First Born Approximation [1BA]. First we introduce 4-Nambu spinors and analyze the familiar BCS theory through this scope. Then we consider a low energy approximation to realize an effective p-wave superconducting 2×2-model from an s-wave superconducting 4×4-model with spin-orbit interaction and Zeeman splitting and analyze the effects of impurities on this model. We introduce impurity potentials and formulate analytic results, through the means of the self-consistent 1BA, of their effect on the systems parameters such as the gap function.

The effects of proximity induced superconductivity in a semiconductor with an externally supplied magnetic field and spin-orbit interactions are intensely studied within the field and there are numerous results quantitatively stating the effect of impurities on such models, see eq. (2.3) below. Two important results for s-wave superconductors are Lutchyn et. al. [8] and Sau et. al. [11]. The former studies the effects of magnetic impurities on the superconductivity induced in a 1D wire and finds a certain robustness. The latter case studies a similar setup but with impurities on the surface of the semiconductor instead which Sau et. al. concludes that the effects of doping can be minimized by increasing the Zeeman splitting compared to the spin-orbit interaction energies.

Where it is possible the formalism we use shall not be restricted to a specific dimension and make use of natural units setting $\hbar = 1$.

As mentioned earlier we wish to modify the BCS theory to also include Rashaba spin-orbit interaction and Zeeman splitting from a magnetic field. First we extend the BCS model to a 4×4 Nambu model to accommodate the possible breaking of time reversal symmetry of the magnetic impurities which will be the first case study of this thesis. For a suitable choice of Nambu spinors[2]

$$\Psi^\dagger(\mathbf{r}) := \begin{pmatrix}\psi^\dagger(\mathbf{r}) & \psi(\mathbf{r})\end{pmatrix} \otimes \begin{pmatrix}\uparrow & \downarrow\end{pmatrix} = \begin{pmatrix}\psi^\dagger_\uparrow(\mathbf{r}) & \psi^\dagger_\downarrow(\mathbf{r}) & \psi_\uparrow(\mathbf{r}) & \psi_\downarrow(\mathbf{r})\end{pmatrix}, \tag{2.1}$$

the 4×4 BCS Hamiltonian is described as follows

$$\mathcal{H}(\mathbf{k}) = \mathcal{H}_0(\mathbf{k}) + \mathcal{H}'(\mathbf{k}) = \xi_\mathbf{k}\tau_3 + \Delta(\mathbf{k})\tau_2\sigma_2. \tag{2.2}$$

The Pauli matrices τ_i and σ_i correspond to particle-hole and spin up-down spaces respectively. The first part describes a free electron gas, $\mathcal{H}_0 = \xi_\mathbf{k}\tau_3$ where $\xi_\mathbf{k} = \frac{\mathbf{k}^2}{2m} - \mu$ is the electron dispersion with mass m and chemical potential μ. The second part describes the superconductivity $\mathcal{H}' = \Delta(\mathbf{k})\tau_2\sigma_2$, where $\Delta(\mathbf{k})$ is the BCS gap function introduced above.

Rashaba spin-orbit interaction stems from the relativistic effect of charged particles (electrons) moving through an electric field. Consider an electron moving through an electric field $\mathbf{E}$, in the electrons stationary frame of reference this corresponds to a magnetic field $\mathbf{B} = -\frac{1}{c^2}\mathbf{v}\times\mathbf{E}$. As the electron has spin it couples to this magnetic field described by the Hamiltonian term $H' = -\mathbf{M}\cdot\mathbf{B} = \left(\frac{g\mu_B}{2}\boldsymbol{\sigma}\right)\cdot\left(\frac{1}{c^2}\mathbf{v}\times\mathbf{E}\right)$. This readily reduces to the form presented below to the one above with an appropriate definition of u. In this model the electric field comes from the atoms of the system which is why it is considered a spin-orbit interaction.

Consider a one dimensional wire which will serve as the main model of concern, in this case we may pick the a specific geometry of the setup. Let the wire lie along the y-axis, the spin orbit interaction in the z direction and the magnetic field to be along the x-direction giving the Hamiltonian

$$\mathcal{H}(k) = \xi_k\tau_3 + \Delta(k)\tau_2\sigma_2 + uk\sigma_3 + B\sigma_2. \tag{2.3}$$

The eigenenergies of this model are

$$E^2_{k\pm} = K^2 + \Delta^2(k) + \xi_k^2 \pm 2\sqrt{K^2\xi_k^2 + B^2\Delta^2(k)}, \tag{2.4}$$

where $K := \sqrt{u^2k^2 + B^2}$. At $k = 0$ the energies are

$$E^2_{0\pm} = B^2 + \Delta_0^2 + \mu^2 \pm 2\sqrt{B^2\mu^2 + B^2\Delta_0^2} \quad \text{or} \quad E_{0\pm} = \left|B \pm \sqrt{\Delta_0^2 + \mu^2}\right|. \tag{2.5}$$

As the chemical potential is known to rapidly decrease at the border of most materials the condition $B^2 > \Delta^2 + \mu^2$ is often called the topological phase. In one dimensional systems this phase can harbor Majorana Fermion states at the end of the wire.

[2] This transforms in to the possibly more familiar basis of pair-time reversed pair, $\Psi^\dagger(\mathbf{r}) = \begin{pmatrix}\psi^\dagger_\uparrow(\mathbf{r}) & \psi^\dagger_\downarrow(\mathbf{r}) & \psi_\downarrow(\mathbf{r}) & -\psi_\uparrow(\mathbf{r})\end{pmatrix}$, through the unitary $U = 1 \oplus i\sigma_y$

We are constrained by the inherent complexity of this model, in that this is nearly impossible to analyze analytically, as is, with Green's functions. So later the approximation $uk \ll B$ is used as the magnetic field is tuned to be very high in these systems. It is however not immediately evident how to implement this approximation. This is exactly the topic of Chapter 2.3 where a so called Schrieffer–Wolff approximation is introduced. A simpler model without spin-orbit interaction or an externally supplied magnetic field can however be solved using Green's function formalism as this is an extension of the BCS model of superconductivity.

2.1 The Self-Consistent First Born Approximation

There are many tools in the physicists phys-belt to deal with disorder in systems. One of them is the Born approximation–the name is slightly misleading as it suggests there is only one, but really it is a diverse complex of approximations. To be as accurate as possible we shall use a self-consistent first Born approximation or SC1BA. The underlying theory stems from deriving Feynman rules governing the impurity potentials, for a full description of this derivation I recommend reading chapter 12 in [3] which this chapter shall be largely based on. The goal is to find the best possible approximate Green's function for a system with discrete impurities. In the Born approximation one introduces the impurity averaged Green's function as the sum over all possible uncorrelated impurity configurations.

The propagator of a system subject to a diagonal single-particle potential $\mathcal{V}$ from point b to point a can be written as the Dyson equation

$$\mathcal{G}(a,b) = \mathcal{G}_0(a,b) + \int \mathcal{G}_0(a,c)\mathcal{V}(c)\mathcal{G}(c,b)\,\mathrm{d}c\,, \tag{2.6}$$

here the labels a, b, c etc. mean points in the phase space of the system, e.g. in position, spin and imaginary time domain these are $a = (\mathbf{r}_a, \sigma_a, \tau_a)$ and the integral is over the domain of this phase space. For time independent potentials, i.e. elastic scattering, the integral over over time can be neglected if the bare Green's function is time translation invariant. Take $\mathcal{V}$ to be a sum of impurity potentials, e.g.

$$\mathcal{V}(\mathbf{r}) = \sum_i u(\mathbf{r} - \mathbf{R}_i), \tag{2.7}$$

where $\mathbf{R}_i$ are uncorrelated and randomly distributed in the system. Using this potential in eq. (2.6) gives equations too complicated to solve exactly but we might hope to solve how this effects a system on average. Define the impurity averaged Green's function as the average of all possible system configurations. Our goal is then to find an expression for this impurity averaged Green's function.

The Born approximation is most elegantly formulated using Feynman diagrams, as such we shall use this as our starting point in this thesis. The impurity averaged Green's function in the Born approximation is defined as the sum of all n-order topologically different diagrams containing $n+1$ propagator lines and p impurities in an unbroken chain scattering off $p \leq n$ impurities exactly n times. Furthermore one should sum over all internal momenta in the diagrams. We may define the self-energy Σ as the impurity averaged Green's function without the external Fermion lines, i.e. we can write it as the following diagrams

$\Sigma(\mathbf{k}, i\omega_n) =$ 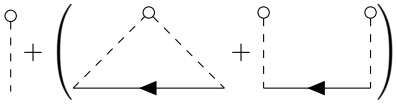 (2.8a)

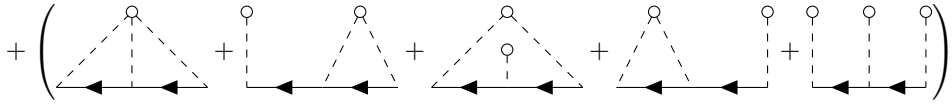 (2.8b)

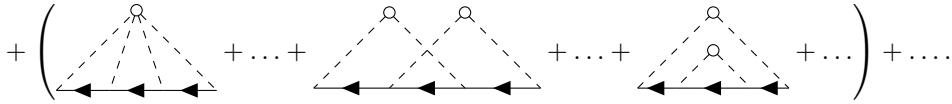 (2.8c)

The Fermion lines denote the pure system, denoted $\mathcal{G}_0$, but in general this does not have to be a 4×4 (or even 2×2) Nambu-Gorkov Green's function. The potential $\mathcal{V}$ may contain internal degrees of freedom, such as atomic spin, which should also average over as by definition the impurity averaged Green's function is the sum of all disorder configurations. The impurity averaged Green's function is labeled $\mathcal{G}$ from here on out.

One often neglects contributions from reducible diagrams, i.e. ones that can be cut into two by removing a single Fermion line, e.g. diagrams 2 and 4 of eq. line (2.8b). Another type of diagram that are often ignored are the crossing diagrams, such as the middle one shown above in eq. line (2.8c). The justification for this is as follows: Consider the non crossing diagram that is the third diagram in eq. line (2.8c). The available phase space of the two internal momenta $\mathbf{k}_1$ and $\mathbf{k}_2$ are hollow hyperspheres of surface width $\Delta k \approx 1/l$ and

radius close to the Fermi momentum, k_F. That is, the phase space $\Omega_{\text{non-crossing}}$ is proportional to the volume of the product the two hyperspheres, which is $(4\pi k_F^2 \Delta k)^2$ in 3D[3]. Meanwhile the crossing diagram, the second diagram in eq. line (2.8c), there is the additional constraint that $|\mathbf{k}+\mathbf{k}_2-\mathbf{k}_1| \approx k_F$ which constrains the momentum transfer to a torus-like shape in the intersection of the two hollow spheres. The volume of this is $\Omega_{\text{crossing}} \propto (4\pi k_F^2 \Delta k)(2\pi k_F \Delta k^2)$. In conclusion the crossing diagram is suppressed relative to the non crossing diagram by a factor of $\Delta k/k_F$. The translation is ofcourse that the product of the average length between scattering events l and the Fermi momentum k_F should be large, or $1/k_F l \ll 1$ for this approximation to be justified. In some doped semiconducting systems this is however not true as the Fermi wavelength is much longer attributed to the comparatively small chemical potential relative to metals. This can lead to an increase in resistivity which is due to weak localization that comes from to these crossing diagrams, see. e.g. [3] Chapter 16.

Returning to the self-energy and the impurity averaged Green's function $\mathcal{G}$. For translation invariant bare systems the Green's function $\mathcal{G}_0(\mathbf{k},\mathbf{k}',i\omega_n)$ is only a function a single momentum $\mathbf{k}$, see Appendix A. Using this assumption and additionally that the impurity averaging should restore translational invariance by Fourier transforming eq. (2.6) into the following (algebraic) Dyson equation

$$\mathcal{G}(\mathbf{k},i\omega_n) = \mathcal{G}_0(\mathbf{k},i\omega_n) + \mathcal{G}_0(\mathbf{k},i\omega_n)\Sigma(\mathbf{k},i\omega_n)\mathcal{G}(\mathbf{k},i\omega_n). \tag{2.9}$$

As the name suggests it is an algebraic equation and can readily be solved by (matrix-) algebraic operations giving

$$\mathcal{G}^{-1}(\mathbf{k},i\omega_n) = \mathcal{G}_0^{-1}(\mathbf{k},i\omega_n) - \Sigma(\mathbf{k},i\omega_n). \tag{2.10}$$

This serves an expression for the impurity averaged Green's function and the only question that remains is how to pick the self-energy Σ. Formally this is written in eq. (2.8) it is impossible for us to sum all of these diagrams. Instead we introduce two of the most common ways to go about determining Σ.

The *First Born Approximation* [1BA] is a first order approximation, taking into account only the simplest diagram describing scattering twice on a single impurity. In the 1BA the self-energy is given by

$$\Sigma^{\text{1BA}}(\mathbf{k},i\omega_n) := \quad \overset{\mathcal{V}(\mathbf{k}-\mathbf{k}')}{\underset{\mathcal{G}_0(\mathbf{k}',i\omega_n)}{\text{ 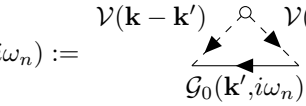 }}} \overset{\mathcal{V}(\mathbf{k}'-\mathbf{k})}{} \quad = \frac{1}{V}\sum_{\mathbf{k}'} \mathcal{V}(\mathbf{k}-\mathbf{k}')\mathcal{G}_0(\mathbf{k}',i\omega_n)\mathcal{V}(\mathbf{k}'-\mathbf{k}). \tag{2.11}$$

This means the (impurity averaged) full Green's function can be written either as

$$\mathcal{G}^{\text{1BA}}(\mathbf{k},i\omega_n) = \mathcal{G}_0(\mathbf{k},i\omega_n) + \mathcal{G}_0(\mathbf{k},i\omega_n)\left[\frac{1}{V}\sum_{\mathbf{k}'} \mathcal{V}(\mathbf{k}-\mathbf{k}')\mathcal{G}_0(\mathbf{k}',i\omega_n)\mathcal{V}(\mathbf{k}'-\mathbf{k})\right]\mathcal{G}_0(\mathbf{k},i\omega_n), \tag{2.12}$$

or found by inverting eq. (2.10) after inserting the expression for the self-energy found in eq. (2.11).

The *self-consistent first Born approximation* [SC1BA] consists of replacing the bare Green's function propagator lines with the impurity averaged Green's function $\mathcal{G}$ to get a self-consistency equation, in the 1BA, by combining eqs. (2.11) and (2.10) to get

$$\Sigma^{\text{SC1BA}}(\mathbf{k},i\omega_n) := \quad \overset{\mathcal{V}(\mathbf{k}-\mathbf{k}')}{\underset{\mathcal{G}(\mathbf{k}',i\omega_n)}{\text{ 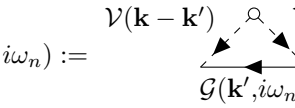 }}} \overset{\mathcal{V}(\mathbf{k}'-\mathbf{k})}{} \quad = \frac{1}{V}\sum_{\mathbf{k}'} \mathcal{V}(\mathbf{k}-\mathbf{k}')\mathcal{G}(\mathbf{k}',i\omega_n)\mathcal{V}(\mathbf{k}'-\mathbf{k}), \tag{2.13}$$

and

$$\mathcal{G}^{-1}(\mathbf{k},i\omega_n) = \mathcal{G}_0^{-1}(\mathbf{k},i\omega_n) - \Sigma(\mathbf{k},i\omega_n) = \mathcal{G}_0^{-1}(\mathbf{k},i\omega_n) - \frac{1}{V}\sum_{\mathbf{k}'} \mathcal{V}(\mathbf{k}-\mathbf{k}')\mathcal{G}(\mathbf{k}',i\omega_n)\mathcal{V}(\mathbf{k}'-\mathbf{k}). \tag{2.14}$$

We say this is the self-consistent equation for $\mathcal{G}$ in the SC1BA. Note that we are still clueless as to the structure of $\mathcal{G}$, and this is an additional assumption one has to intuit into the formalism. In the SC1BA the self-energy can be written diagrammatically

$$\Sigma(\mathbf{k},i\omega_n) = \quad \text{ 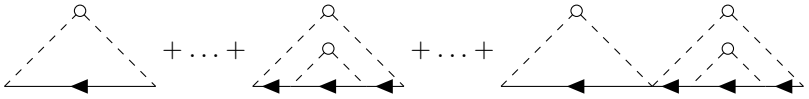 } \quad + \ldots \tag{2.15}$$

[3]Although this argument is very dimension sensitive one can easily be convinced that the dimension of the phase space of crossing diagrams is always one lower than the non-crossing ones.

That is all the sum of all possible combinations of these *wigwam* tents, i.e. of the form in eq. (2.11), either next to eachother or under one another. Here the Fermion propagator lines represent the bare Green's function $\mathcal{G}_0$.

For example we might take the Green's function of the *free electron model*

$$\mathcal{G}_0(\mathbf{k}, i\omega_n) = \frac{1}{i\omega_n - \xi_{\mathbf{k}}}, \tag{2.16}$$

where $\xi_{\mathbf{k}} = \frac{k^2}{2m} - \mu$, m is the electron mass and μ is the chemical potential. Then a parametrization of the *renormalized* Green's function $\mathcal{G}$ under some impurity potential $\mathcal{V}$, may be taken to be

$$\mathcal{G}(\mathbf{k}, i\omega_n) = \frac{1}{i\tilde{\omega}_n - \tilde{\xi}_{\mathbf{k}}} \quad \text{where} \quad \tilde{\xi}_{\mathbf{k}} = \frac{k^2}{2\tilde{m}} - \tilde{\mu}. \tag{2.17}$$

Here the 'guess' consists of making the *renormalized* frequencies $i\tilde{\omega}_n$ and dispersion $\tilde{\xi}_{\mathbf{k}}$ look like similar functions of $\mathbf{k}$ as the originals. This is not an exact science but as we shall see below for $\delta(r)$-like impurity potentials these choices will suffice. For the free electron gas the self-consistent equation is

$$[i\tilde{\omega}_n - \tilde{\xi}_{\mathbf{k}}]^{-1} = [i\omega_n - \xi_{\mathbf{k}}]^{-1} - \frac{1}{V}\sum_{\mathbf{k}'} \mathcal{V}(\mathbf{k} - \mathbf{k}')[i\tilde{\omega}_n - \tilde{\xi}_{\mathbf{k}'}]^{-1}\mathcal{V}(\mathbf{k}' - \mathbf{k}). \tag{2.18}$$

2.2 The Effect of Disorder on the BCS Superconductor

As an example let us apply this newfound Born approximation to the BCS Hamiltonian that serves as a basis for the model in eq. (2.3). We might ask ourselves what is the effect of impurities in the superconductor? Physically there could be disorder from an imperfect the manufacturing process of superconductor giving rise to low density impurities. The effect of such impurities may or may not depend on the spin polarization of the atoms involved as such our model shall take into account this distinction. For now the dimensionality of the system is arbitrary meaning constraining to the one dimensional wire geometry comes later. Motivated by this discussion we define the impurity potential in the Nambu basis stated in eq. (2.1) at the start of this chapter

$$\mathcal{Y}(\mathbf{r}) := V\tau_3 \sum_i \delta(\mathbf{r} - \mathbf{R}_i) + \boldsymbol{\alpha} \cdot W \sum_\beta \mathbf{S}_\beta \delta(\mathbf{r} - \mathbf{R}_\beta) \quad \text{where} \quad \boldsymbol{\alpha} = \sigma_2\mathbf{j} + \tau_3(\sigma_1\mathbf{i} + \sigma_3\mathbf{k}), \tag{2.19}$$

where $\mathbf{S}_\beta$ is the disorder spin operator at site β and V, W are the strength of the impurities, here assumed constant for all impurities. $\mathbf{R}_i$ and $\mathbf{R}_\beta$ are the positions of the spinless and spinful impurities respectively. For clarity we define the spinless and spinful parts independently

$$\mathcal{V}(\mathbf{r}) := V\tau_3 \sum_i \delta(\mathbf{r} - \mathbf{R}_i) \quad \text{and} \quad \mathcal{W}(\mathbf{r}) := \boldsymbol{\alpha} \cdot W \sum_\beta \mathbf{S}_\beta \delta(\mathbf{r} - \mathbf{R}_\beta). \tag{2.20}$$

Although these might have a strange form to those unfamiliar with the Nambu formalism, $\mathcal{V}(\mathbf{r})$ is just a *Dirac Comb* like potential acting on both particles and holes of the system while $\mathcal{W}(\mathbf{r})$ represents spin operators located at all the points R_β. Transforming to $k-$space the impurity potential takes the form

$$\mathcal{Y}(\mathbf{k}) = \begin{pmatrix} v_{\mathbf{k}} + w_{3,\mathbf{k}} & w_{1,\mathbf{k}} - iw_{2,\mathbf{k}} & 0 & 0 \\ w_{1,\mathbf{k}} + iw_{2,\mathbf{k}} & v_{\mathbf{k}} - w_{3,\mathbf{k}} & 0 & 0 \\ 0 & 0 & -v_{\mathbf{k}} - w_{3,\mathbf{k}} & -w_{1,\mathbf{k}} - iw_{2,\mathbf{k}} \\ 0 & 0 & -w_{1,\mathbf{k}} + iw_{2,\mathbf{k}} & -v_{\mathbf{k}} + w_{3,\mathbf{k}} \end{pmatrix}, \tag{2.21}$$

where $v_{\mathbf{k}}$ and $u_{i,\mathbf{k}}$ are the Fourier transformations of the spinless and spinful potential parts, as in eq. (2.20):

$$v_{\mathbf{k}} = V\sum_i e^{-i\mathbf{k}\cdot\mathbf{R}_i} \quad \text{and} \quad w_{i,\mathbf{k}} = W\sum_\beta S_{i,\beta} e^{-i\mathbf{k}\cdot\mathbf{R}_\beta}. \tag{2.22}$$

In the 1BA the first order diagrams can be split up into two separate scattering events as shown in Figure 1 below. From this we see the self-energy is

$$\begin{aligned} \Sigma(\mathbf{k}, i\omega_n) &= \frac{1}{V}\sum_{\mathbf{k}'}(\mathcal{V}(\mathbf{k} - \mathbf{k}')\mathcal{G}(\mathbf{k}', i\omega_n)\mathcal{V}(\mathbf{k}' - \mathbf{k})) + \frac{1}{V}\sum_{\mathbf{k}'}\langle(\mathcal{W}(\mathbf{k} - \mathbf{k}')\mathcal{G}(\mathbf{k}', i\omega_n)\mathcal{W}(\mathbf{k}' - \mathbf{k})\rangle_S \\ &= \frac{1}{V}\sum_{\mathbf{k}'} |v_{\mathbf{k}-\mathbf{k}'}|^2 \tau_3\mathcal{G}(\mathbf{k}', i\omega_n)\tau_3 + \frac{1}{V}\sum_{\mathbf{k}'ij}\langle w_{i,\mathbf{k}-\mathbf{k}'}\alpha_i\mathcal{G}(\mathbf{k}', i\omega_n)w_{j,\mathbf{k}'-\mathbf{k}}\alpha_j\rangle_S \\ &= N_i|V|^2\frac{1}{V}\sum_{\mathbf{k}'}\tau_3\mathcal{G}(\mathbf{k}', i\omega_n)\tau_3 + \frac{1}{3}S(S+1)N_\beta|W|^2\frac{1}{V}\sum_{\mathbf{k}'i}\alpha_i\mathcal{G}(\mathbf{k}', i\omega_n)\alpha_i, \end{aligned} \tag{2.23}$$

here $\langle - \rangle_S$ is the average of the impurity spins and $\langle S^i_\beta S^j_\beta \rangle_S = \frac{1}{3}S(S+1)\delta_{ij}$, i.e. the disorder is assumed paramagnetic.

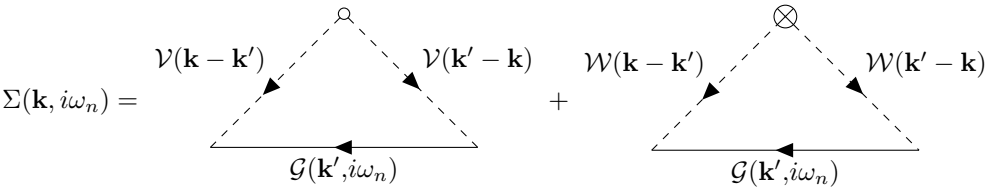

Figure 1: Feynman diagram scattering on the two types of impurities: spinless and spinful, represented by vertices $\circ$ and $\otimes$ respectively. Notice how in the self-consistent approach the impurity averaged Green's function, $\mathcal{G}$, for the internal propagator.

With the self-energy as in 1 the diagramatic series expand this in a similar fashion as above in eq. (2.15),

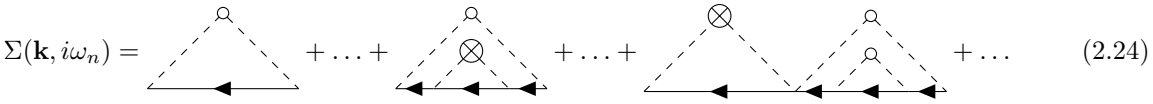

(2.24)

Here the Fermion propagator lines represent the bare Green's function $\mathcal{G}_0$.

It is common practice within self-consistent approximations to parametrize the impurity averaged Green's Function in the self-consistent approximation in terms of some coefficient functions as it can be (uniquely up to a choice of basis) expressed by some linear combination of the basis elements of $SU(2)^{\otimes 2}$. One should easily be convinced all but the elements chosen bellow should be zero

$$\mathcal{G}^{-1}(\mathbf{k}, i\omega_n) = \mathcal{G}_0^{-1}(\mathbf{k}, i\omega_n) - \Sigma(\mathbf{k}, i\omega_n) = i\tilde{\omega}_n - \tilde{\xi}_{\mathbf{k}}\tau_3 - \tilde{\Delta}(\mathbf{k})\tau_2\sigma_2. \tag{2.25}$$

Solving this self-consistent equation provide coupled equations for $\tilde{\Delta}$ and $i\tilde{\omega}_n$ including terms of Δ and $i\omega_n$. In case of an isotropic singlet gap, $\Delta_S(\mathbf{k}) = \Delta$ and $\tilde{\Delta}_S(\mathbf{k}) = \tilde{\Delta}$, and quasi particle spectrum $\xi_{\mathbf{k}} = \mathbf{k}^2/2m - \mu$, the structure of these integrals are very similar to the ones found in Appendix D. In eq. (2.23) change the sum over $\mathbf{k}$ to an integral over $\mathbf{k}$, this can in turn be exchanged for an integral over ξ and the integrand is the derivative of an arctan function. From this argument, using eq. (2.25), we find equations

$$-\frac{1}{V}\sum_{\mathbf{k}} \mathcal{G}(\mathbf{k}, i\omega_n) = \int_{\mathbb{R}^d} \frac{i\tilde{\omega}_n + \tilde{\xi}_{\mathbf{k}}\tau_3 + \tilde{\Delta}\tau_2\sigma_2}{(2\pi)^d(\tilde{\omega}_n^2 + \tilde{\xi}_{\mathbf{k}}^2 + \tilde{\Delta}^2)}\,\mathrm{d}\mathbf{k} = \frac{d_n(0)}{(2\pi)^d}\int_{\mathbb{R}} \frac{i\tilde{\omega}_n + \tilde{\Delta}\tau_2\sigma_2}{\tilde{\omega}_n^2 + \tilde{\xi}^2 + \tilde{\Delta}^2}\,\mathrm{d}\xi = \frac{\pi d_n(0)}{(2\pi)^d}\frac{i\tilde{\omega} + \tilde{\Delta}\tau_2\sigma_2}{\sqrt{\tilde{\omega}_n^2 + \tilde{\Delta}^2}}. \tag{2.26}$$

Here $d_n(0)$ is the normal state density of states at the Fermi level, that is when changing the integral a density of states appear $d_n(\epsilon)$ and is approximated as a constant at the Fermi level. Then, by combining eqs. (2.23), (2.25) and (2.26), in general,

$$(i\omega_n - i\tilde{\omega}_n) - (\xi_{\mathbf{k}} - \tilde{\xi}_{\mathbf{k}})\tau_3 - (\Delta - \tilde{\Delta})\tau_2\sigma_2 = -\frac{1}{2}\frac{1}{\tau_i}\frac{\tilde{\omega}_n - \tilde{\Delta}\tau_2\sigma_2}{\sqrt{\tilde{\omega}_n^2 + \tilde{\Delta}^2}}\frac{1}{(2\pi)^{d-1}} - \frac{1}{2}\frac{1}{\tau_\beta}\frac{\tilde{\omega}_n + \tilde{\Delta}\tau_2\sigma_2}{\sqrt{\tilde{\omega}_n^2 + \tilde{\Delta}^2}}\frac{1}{(2\pi)^{d-1}}, \tag{2.27}$$

where the parameters of the spinless and spinful impurities are defined respectively

$$\tau_i^{-1} := N_i|V|^2 d_n(0) \quad \text{and} \quad \tau_\beta^{-1} := \frac{1}{3}S(S+1)N_\beta|W|^2 d_n(0). \tag{2.28}$$

Reducing eq. (2.27) into component wise 6equations, for a 1D wire this gives the following self-consistent equations

$$\tilde{\omega}_n = \omega_n + \frac{1}{2}\left(\frac{1}{\tau_i} + \frac{1}{\tau_\beta}\right)\frac{\tilde{\omega}_n}{\sqrt{\tilde{\omega}_n^2 + \tilde{\Delta}^2}} \quad \text{and} \quad \tilde{\Delta} = \Delta + \frac{1}{2}\left(\frac{1}{\tau_i} - \frac{1}{\tau_\beta}\right)\frac{\tilde{\Delta}}{\sqrt{\tilde{\omega}_n^2 + \tilde{\Delta}^2}}. \tag{2.29}$$

These are well known results, see e.g. Rickayzen [10]. Solving these equations analytically is virtually impossible, but a numerical solution is readily obtained. As explained in Appendix D doing a Wick rotation and taking the imaginary part gives the density of states

$$\frac{d_s(\omega)}{d_n(0)} = \mathrm{Re}\frac{\tilde{\omega}}{\sqrt{\tilde{\omega}^2 - \tilde{\Delta}^2}}. \tag{2.30}$$

Solving eqs. (2.29) and plotting the density of states one obtains graphs such as shown in Fig. 2 below.

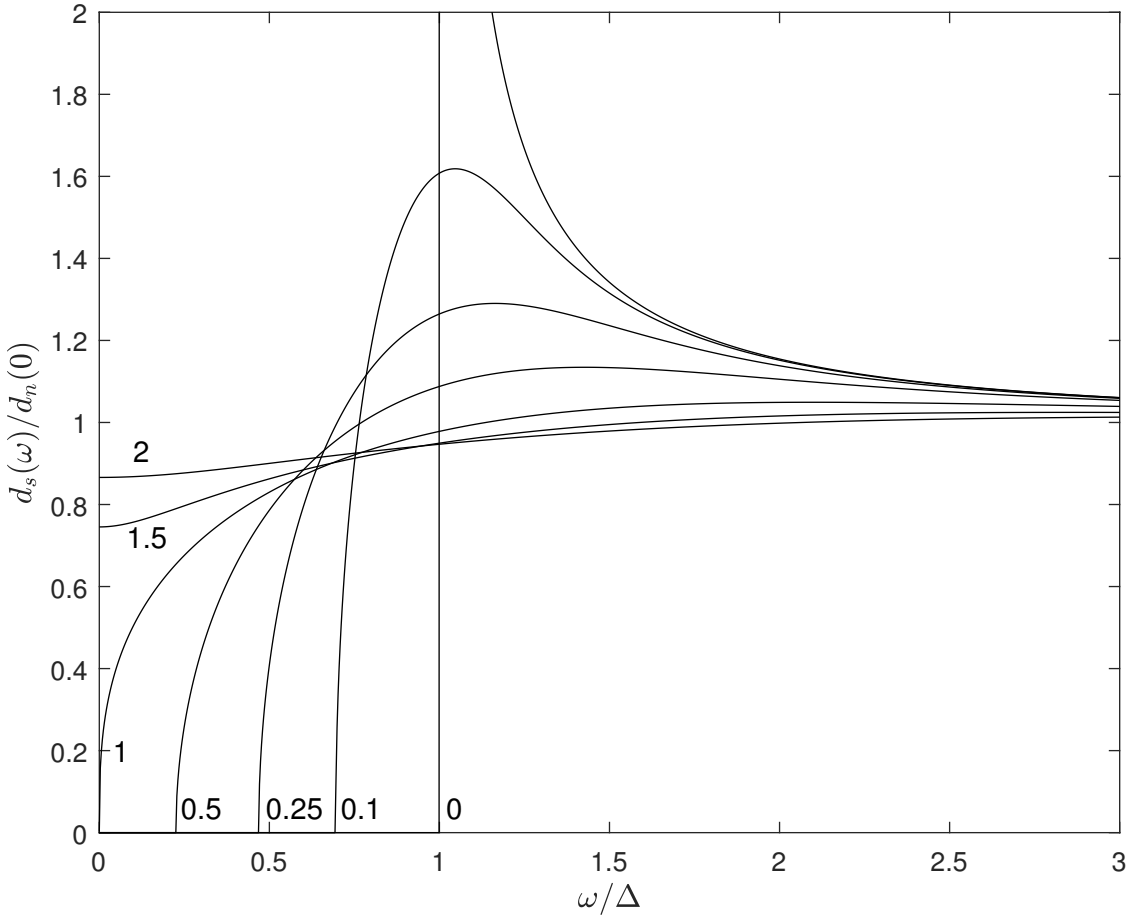

Figure 2: Plot of the normalized density of states for a superconducting system with different disorder strengths. The disorder strength τ_β^{-1} goes from 0 to 2Δ as indicated near the graphs. Non-magnetic impurities are not considered here, see main text for more detail. Note this is based on numerical simulation rather than analytics.

In Fig. 2 the density of states varies as τ_β^{-1} is increased. Interestingly we still see *hard gap*, i.e a region where the density of states is zero, for non-zero disorder. This is not entirely what one would expect using other approximation schemes. One such example is found with the Coherent Potential Approximation in an article by Hlubina et. al. [4]. They find this hard gap to disappear with any added disorder and a soft gap to remain as the frequency is broadened by the characteristic disorder. In SC1BA this hard gap closes completely when τ_β^{-1} is of similar magnitude as the gap Δ. This is not indicative of a complete destruction of the superconducting state[4]. For $\tau_\beta^{-1} > \Delta$ there are still soft peaks at increasingly larger frequencies ω/Δ. In the limit $\tau_\beta^{-1} \to \infty$ the density of states goes to one, $d_s(\omega)/d_n(0) \to 1$ as we would expect. This means for strong magnetic disorder the DOS of the model returns to that of the free electron gas.

Although not displayed on the plot one can vary τ_i^{-1} independently of τ_β^{-1} to find the self-consistent solutions to be completely independent of τ_i^{-1}. That is, for any τ_i^{-1}, varying τ_β^{-1} one would obtain the same plot as in Fig. 2. This is in compliance with *Anderson's theorem* which simply states that, namely that conventional superconductors, such as the BCS theory, are robust with respect to non-magnetic disorder. As such, if τ_β^{-1} is set to 0 and τ_i^{-1} is varied arbitrarily one always obtains the BCS DOS, labeled by 0 on the figure.

On a final note before moving on, let's briefly touch on the dimensionallity of the system. For higher than 1D note that the parameters τ_i^{-1} and τ_β^{-1} in eq. (2.29) can be exchanged for new, dimension dependent, $\tilde{\tau}_{i,d}^{-1}$ and $\tilde{\tau}_{\beta,d}^{-1}$, in relation as follows

$$\tilde{\tau}_{i,d}^{-1} := \tau_i^{-1}(2\pi)^{d-1} \quad \text{and} \quad \tilde{\tau}_{\beta,d}^{-1} := \tau_\beta^{-1}(2\pi)^{d-1}. \tag{2.31}$$

[4]This can be investigated by solving the self-consistent equation for the BCS order parameter defined above or in Appendix C

That is, a 2D plane superconductor is more robust to disorder by a factor of 2π and a 3D superconductor is further more robust to disorder by a factor of 2π compared to the 2D plane and $(2\pi)^2$ compared to the 1D wire.

In the case of a 1D-wire[5] the solutions may be obtained exactly by taking into account the renormalization of the dispersion ξ_k. These integrals are significantly more difficult and we shall only cover them in part here, but the full solutions can be found in Appendix B. In summary in this exact methodology do not use ξ integrals and instead calculate the Green's function directly from the k-integral using a suitable choice of contour. As is shown in Appendix B, the Green's function $\mathcal{G}_0(0,0,i\omega_n)$ can be parametrized in terms of functions f_n, g_n, h_n as

$$\mathcal{G}_0(0,0,i\omega_n) = \frac{1}{L}\sum_k \mathcal{G}_0(k,i\omega_n) = \int_{\mathbb{R}} \mathcal{G}_0(k,i\omega_n)\frac{\mathrm{d}k}{2\pi} = -f_n\left[(i\omega_n + \Delta\tau_2\sigma_2)h_n + g_n\tau_3\right]. \tag{2.32}$$

These functions f_n, g_n, h_n will depend on the system parameters $i\omega$, μ and Δ and their mutual relations as this will influence the specifics of the contour integral in k. It turns out one of these so called *parameter regimes* dominate the others and is the most common. In this case the functions f_n, g_n, h_n take the form

$$f_n := \frac{i}{8mS_+S_-\sqrt{\Delta^2-\omega_n^2}}, \quad g_n := (R_+-\mu)S_-^1 + (R_--\mu)S_+^1 \quad \text{and} \quad h_n := S_- + S_+, \tag{2.33}$$

where $S_\pm$ and $R_\pm$ are the roots of respectively k and $\epsilon = \frac{k^2}{2m}$ in the denominator of $\mathcal{G}(k,i\omega_n)$ in eq. (2.32), that is $S_\pm = \sqrt{\mu \pm \sqrt{\Delta^2-\omega_n^2}}$. Furthermore parametrizing the impurity averaged Green's function as above

$$\mathcal{G}^{-1}(k,i\omega_n) = i\tilde{\omega}_n - \tilde{\xi}_{\mathbf{k}}\tau_3 - \tilde{\Delta}(\mathbf{k})\tau_2\sigma_2 \quad \text{where} \quad \tilde{\xi}_k = \frac{k^2}{2m} - \tilde{\mu} \quad \text{and} \quad \tilde{\Delta}(k) = \tilde{\Delta}, \tag{2.34}$$

and using the same integral formalism as was used with $\mathcal{G}_0$, it takes the form

$$\mathcal{G}(0,0,i\omega_n) = \frac{1}{L}\sum_k \mathcal{G}(k,i\omega_n) = \int_{\mathbb{R}} \mathcal{G}(k,i\omega_n)\,\mathrm{d}k = -\tilde{f}_n[(i\tilde{\omega}_n + \tilde{\Delta}\tau_2\sigma_2)\tilde{h}_n + \tilde{g}_n\tau_3]. \tag{2.35}$$

Here the tilde on the functions $\tilde{f}_n, \tilde{g}_n, \tilde{h}_n$ mean they have a similar structure as eq. (2.33), but are evaluated in the renormalized parameters, e.g. $S_\pm = \sqrt{\tilde{\mu} \pm \sqrt{\tilde{\omega}_n^2 + \tilde{\Delta}^2}}$. Once again this can be put into eq. (2.23) to find the self-consistent equation

$$(i\omega_n - i\tilde{\omega}_n) - (\xi_k - \tilde{\xi}_k)\tau_3 - (\Delta - \tilde{\Delta})\tau_2\sigma_2 = -\frac{1}{\tau_i}\tilde{f}_n[(i\tilde{\omega}_n - \tilde{\Delta}\tau_2\sigma_2)\tilde{h}_n + \tilde{g}_n\tau_3] - \frac{1}{\tau_\beta}\tilde{f}_n[(i\tilde{\omega}_n + \tilde{\Delta}\tau_2\sigma_2)\tilde{h}_n + \tilde{g}_n\tau_3]. \tag{2.36}$$

The definitions of τ_i^{-1} and τ_β^{-1} are as before

$$\tau_i^{-1} := N_i|V|^2 \quad \text{and} \quad \tau_\beta^{-1} := \frac{1}{3}S(S+1)N_\beta|W|^2. \tag{2.37}$$

Breaking down eq. (2.36) component-wise we see that the mass cannot be renormalized using the Dirac delta impurity potentials, as the above expression must be true for all k, thus justifying the choice of renormalized dispersion $\tilde{\xi}_k = \frac{k^2}{2m} - \tilde{\mu}$. Furthermore we find component wise self-consistent equations for the 3 system parameters

$$i\tilde{\omega}_n = i\omega_n + \tilde{f}_n\tilde{h}_n\left[\frac{1}{\tau_i} + \frac{1}{\tau_\beta}\right]i\tilde{\omega}_n, \quad \tilde{\mu} = \mu + \tilde{f}_n\tilde{g}_n\left[\frac{1}{\tau_i} + \frac{1}{\tau_\beta}\right] \quad \text{and} \quad \tilde{\Delta} = \Delta + \tilde{f}_n\tilde{h}_n\left[\frac{1}{\tau_i} - \frac{1}{\tau_\beta}\right]\tilde{\Delta}. \tag{2.38}$$

These self-consistent equations are of a similar structure to eqs. (2.29) found above. These equations a monumentally difficult if not impossible to solve analytically so we instead turn to numerical simulations. Once the solutions to the renormalized parameters are found they can be inserted into the density of states, which can be written as

$$d_s(\omega) = -\lim_{\eta\to 0}\mathrm{Im}[\mathcal{G}(0,0,\omega+i\eta)] = \lim_{\eta\to 0}\mathrm{Im}[\tilde{f}(\tilde{\omega})(\tilde{\omega}\tilde{h}(\tilde{\omega}) + \tilde{g}(\tilde{\omega})\tau_3)]. \tag{2.39}$$

For different values of τ_β^{-1} the DOS is plotted in Figure 3 below.

[5] And technically also in the case a 2D-plane geometry. Although this is only possible when considering the nonlocal GF, that is $\mathcal{G}_0(0,0,i\omega_n)$.

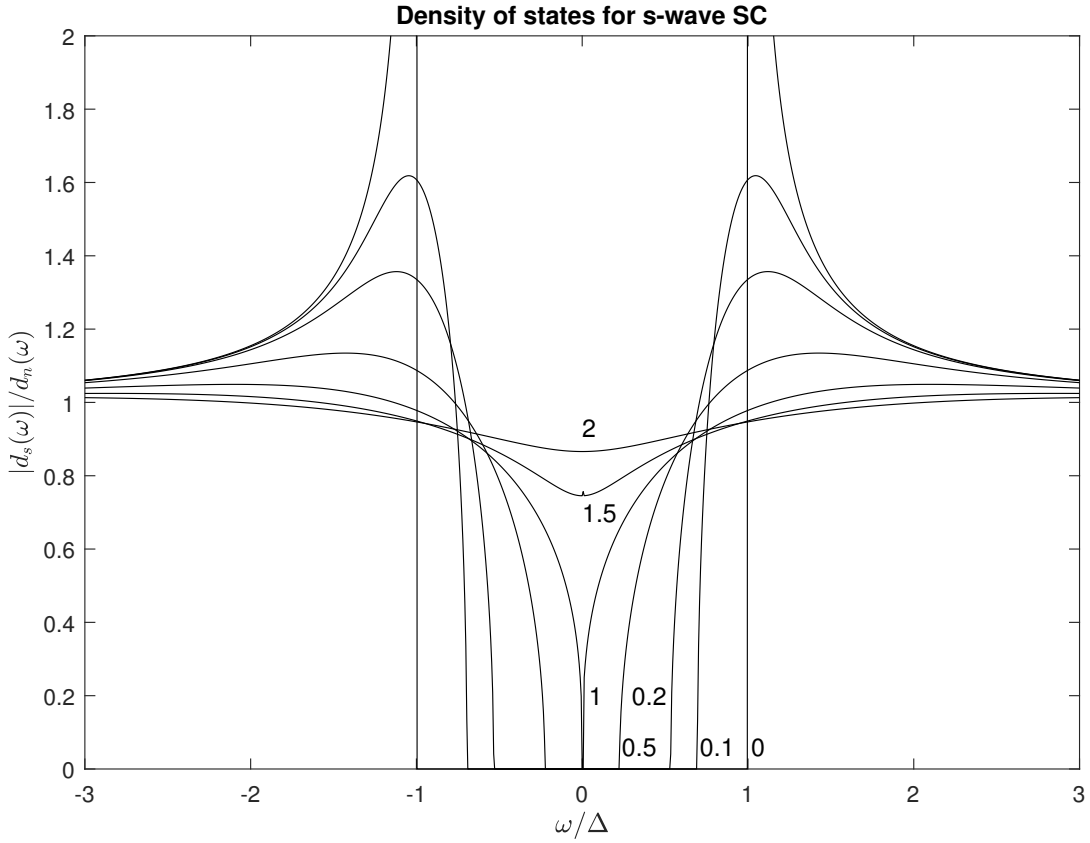

Figure 3: Plot of the normalized density of states for a superconducting system with different disorder strengths. The disorder strength τ_β^{-1} go from 0 to 2 as indicated near the graphs and the relation between the gap and chemical potential is $\mu/\Delta = 10^4$. Non-magnetic impurities are not considered here, see the main text for more detail.

At first glance Fig. 3 is very similar to Fig. 2 discussed earlier, and as such might not seem noteworthy. But this is exactly what is so impressive about the plot! Even after going through all the trouble of solving the k-space integrals exactly the solutions are similar to those found by the constant density of states approximation. So in actuality the similarity between Figs. 3 and 2 is a testimony to the effectiveness of this approximation. The ratio between the chemical potential and gap $\mu/\Delta = 10^4$ is the determining factor in this, however this resemblance remains even for relatively small fractions μ/Δ.

The impurity parameter τ_β^{-1} goes from 0 to 2 in units of the magnitude of $\Delta\sqrt{8m^3\mu}$. This characteristic scale was found semi-experimentally, i.e. it is defined as the point at which the hard gap closes completely and *inferred* by varying the parameters of the numerical simulation–both independently and codependently.

The superconducting density of states has been normalized against the normal state density of states $d_n(\omega)$, which may be found by setting $\Delta = 0$ in the Green's function or in eq. (2.39). There are ofcourse singularities in the normal state DOS at $\omega = -\mu$ but for large μ these have minuscule influence on the plotted DOS in Fig 3. Furthermore the model obeys Anderson's theorem for all values of τ_β^{-1} and appear unchanged as $\tau_\beta^{-1} = 0$. Particularly for $\tau_\beta^{-1} = 0$, $\frac{d_s(\omega)}{d_n(\omega)}$ resembles the BCS density of states for all τ_i^{-1}.

As an aside consider how the parameters are renormalized. The numerical solution to the renormalized parameters as dictated by the self-consistent equations can be summarized loosely as broadening them by some small imaginary part while their real part remain mostly untouched. This statement is really about the self-energy through the relation $\Sigma = \mathcal{G}_0^{-1} - \mathcal{G}^{-1}$, i.e. the real part of Σ is comparatively small compared to its imaginary part–except for inside the hard gap.

One additional feature of doing the integrals in the self-energy in k-space instead of changing to ξ is that it allows us to analyze the small μ limit. Physically this occurs in semiconductors or it can be induced by manipulating the electric potential of the system. However we may still consider what happens with the density of states for the s-wave superconductor of the extended BCS formalism discussed above. The results of the self-consistent Born analysis is plotted in Fig. 4 below.

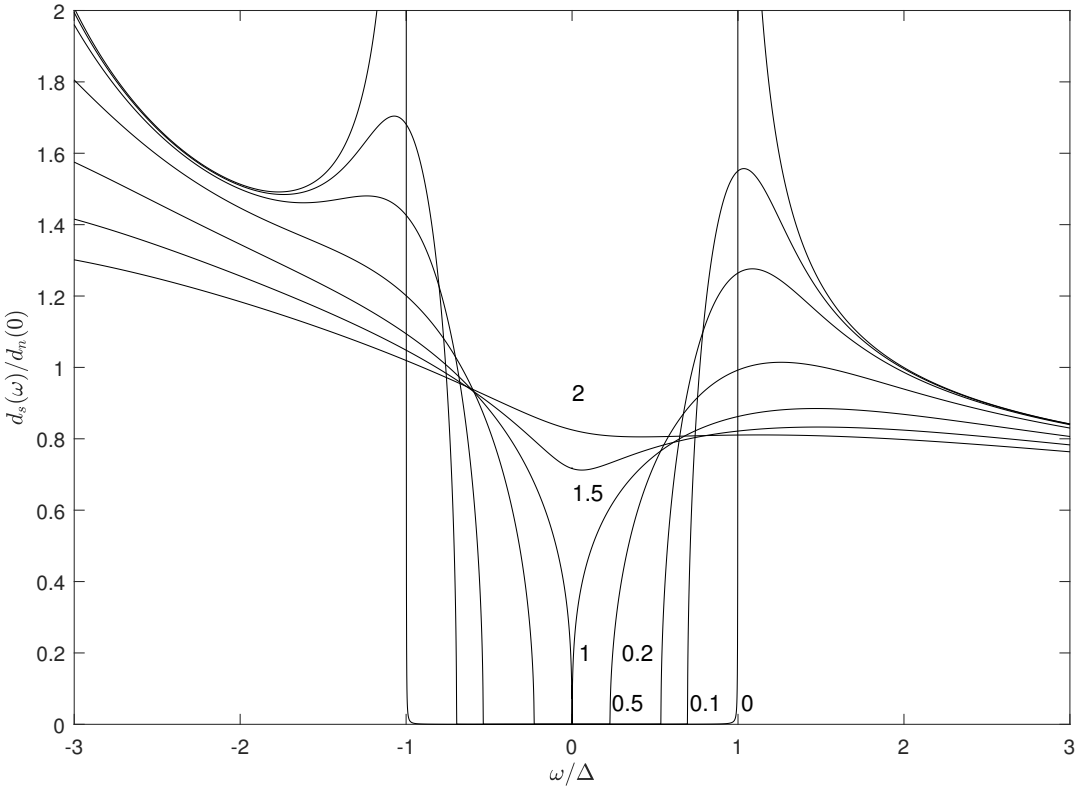

Figure 4: Plot of the normalized electron density of states for a superconducting system with different disorder strengths. The disorder strength τ_β^{-1} go from 0 to 2 similarly to Fig. 3 but with the relation between the gap and chemical potential is $\mu/\Delta = \sqrt{15}$. The frequencies is broadened by a factor $i\eta = i10^{-4}$. Non-magnetic impurities are not considered here, see main text for more detail.

By comparing Figs. 3 and 4 the structure of d_s becomes slightly more slanted as μ is decreased. This effect comes from the two additional singularities in d_s attributed to the function f_n in eq. (2.33) at $\omega = \pm\sqrt{\Delta^2+\mu^2}$– more on this later. Beyond these singularities d_s vanish rapidly as $\omega^{-1/2}$ to the right and becomes heavily suppressed to the left of $-\sqrt{\Delta^2+\mu^2}$. When μ and Δ are relatively close the normal state density of states $d_n(\omega)$ has a non-constant structure close to the gap and serves as a poor normalization factor so the DOS at the Fermi level $d_n(0)$ is used instead. This allows us to make meaningful comments on the structure of the superconducting DOS for increasingly small μ. Note also the disorder has much a similar effect as for large μ with the exception of where the influence of a modified Van Hove peak at $\omega = -\sqrt{\Delta^2+\mu^2}$ is boardened by the impurities.

Plots in extended frequency space is shown in Fig. 5 below. Here we see the effects of different disorder strengths on the DOS for low filings $\mu/\Delta = \sqrt{15}$. For very low densities we see the general structure of $d_s(\omega)$ is retained but the singularity peaks at $\omega = -\sqrt{\Delta^2+\mu^2}, -\Delta, \Delta, \sqrt{\Delta^2+\mu^2}$ are smeared out. The peak at $\omega = \sqrt{\Delta^2+\mu^2}$ comes as a surprise: in the normal state there is only a singularity at $\omega = -\mu$, the Van Hove peak. However in the superconducting state there are the coherence peaks at $\omega = \pm\Delta$ and a modified Van Hove peak at $\omega = -\sqrt{\Delta^2+\mu^2}$ and finally *the phantom peak* at $\omega = \sqrt{\Delta^2+\mu^2}$. I am hesitant to write this off as a numerical error as this is a genuine solution to the self-consistent equations and the peak is broadened once disorder is added, see e.g. the bottom right of Fig. 5 (a). Note that the phantom peak is narrowed as Δ is decreased compared to the three other singularities which are mostly unphased by such changes. The nature of this phantom peak remains unanswered.

The left most singularity, at $\omega = -\sqrt{\Delta^2+\mu^2}$ is smeared out for increasing disorder strengths but retain the structure similar to the bottom left of Fig. 5 (a). That is: there exists some point $\omega_p < -\sqrt{\Delta^2+\mu^2}$ for which $d_s(\omega)$ vanishes, and this point moves further to the left as τ_β^{-1} is increased. In the normal state this point corresponds to $-\mu$ and for frequencies smaller than this there are no occupied states.

In the limit where $\mu \to 0$ the Van Hove peak approach the coherence peaks of the superconductor. In this case the DOS is zero below $\omega = -\Delta$ for no impurities, but as impurities are added the coherence peak is broadened and fill some of these states. From the above discussion we can think of this as initially taking ω_p to

be $-\Delta$ and then decreasing ω_p as impurities are added to the system. For example in Fig. 5 (a) $\omega_p/\Delta \approx -4$ for $\tau_\beta^{-1} = 0$ and $\omega_p/\Delta \approx -4.5$ for $\tau_\beta^{-1} = 0.1$.

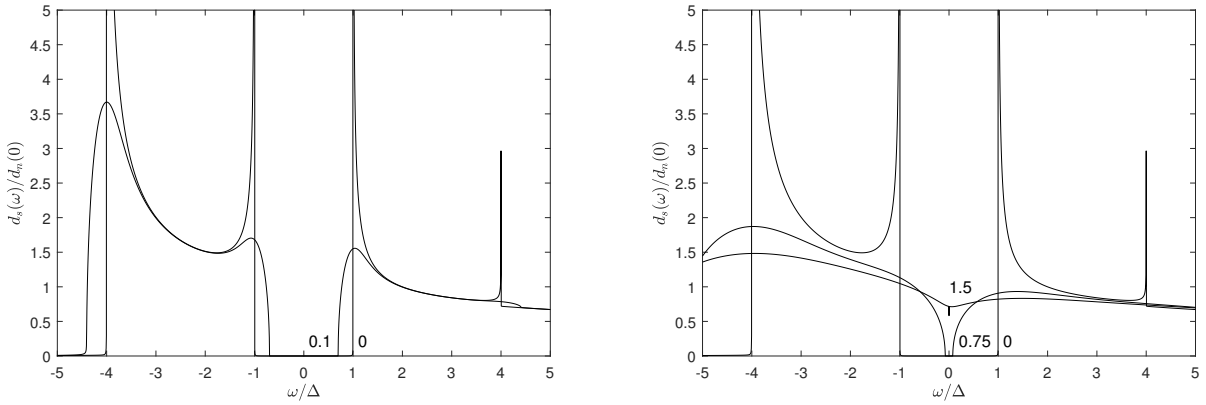

(a) Effect of low density impurities on the DOS.

(b) Effect of high density impurities on the DOS.

Figure 5: DOS at different impurities at a low filling $\mu/\Delta = \sqrt{15}$. A broadening of the frequency ω was imposed as $i\eta = i10^{-4}$. Fig. (a): the disorder strength τ_β^{-1} goes from 0 to 0.1 in units of $\Delta\sqrt{8m^3\mu}$. Fig. (b): the disorder strength τ_β^{-1} goes from 0 to 1.5 in units of $\Delta\sqrt{8m^3\mu}$. Note there is a single point with numerical error at $\omega = 0$ for the DOS with impurity strength $\tau_\beta^{-1} = 1.5$.

So far the topic of discussion has only considered the electron DOS; a few remarks on the hole DOS is in order. In the limit $\mu \to \infty$ the electron and hole DOS are the same, see eq. (2.30), as the τ_3 component is integrated out. Doing the integrals in k-space allows us to distinguish the DOS of the electrons from the holes. This resemblance remain for large μ, but not infinite, in our model as seen in Fig. 3. The relationship between the electron DOS $d_s^e(\omega)$ and hole DOS $d_s^h(\omega)$ is $d_s^e(\omega) = -d_s^h(-\omega)$ which follows directly from eq. (2.39).

2.3 A Low Energy Schrieffer-Wolff Approximation and p-wave Superconductivity

In the previous chapter we succeeded in generalizing the BCS DOS and stating the influence of disorder in such a superconductor. When attempting to apply the First Born Approximation scheme to the full model of the Hamiltonian of eq. (2.3), one has trouble finding the Green's function $\mathcal{G} = (i\omega_n - \mathcal{H})^{-1}$. This is because of the inherent complexity of the model. One way to circumvent this rather tedious problem is to use a standard method of reducing the problem to a low energy model. In layman terms this is done by diagonalizing the normal state Hamiltonian, $\mathcal{H}_0 + \mathcal{H}''$, and making an expansion for the full Hamiltonian $\mathcal{H}$ in $\mathcal{H}'$ in this diagonal basis and finally projecting the result onto the low energy basis. For a thorough introduction to this methodology see [2].

First off some important preliminary definitions and discussion is in order. Recall the full Hamiltonian also includes the BCS gap function δ, here assumed constant, and takes the form

$$\mathcal{H}(k) = \begin{pmatrix} \xi_k + uk & -iB & 0 & \delta \\ iB & \xi_k - uk & -\delta & 0 \\ 0 & -\delta & -\xi_k + uk & -iB \\ \delta & 0 & iB & -\xi_k - uk \end{pmatrix}. \tag{2.40}$$

As $\mathcal{H}_0$ and $\mathcal{H}''$ do not mix particles and holes they are block diagonal in 4-Nambu space. Motivated by this, define the block Hamiltonians for particles and holes, $\mathcal{H}_e$ and $\mathcal{H}_h$, respectively, so that:

$$\mathcal{H}_0 + \mathcal{H}'' = \begin{pmatrix} \mathcal{H}^e & 0 \\ 0 & \mathcal{H}^h \end{pmatrix} \quad \text{where} \quad \mathcal{H}_e = \begin{pmatrix} \xi_k + uk & -iB \\ iB & \xi_k - uk \end{pmatrix} \quad \text{and} \quad \mathcal{H}_h = \begin{pmatrix} -\xi_k + uk & -iB \\ iB & -\xi_k - uk \end{pmatrix}. \tag{2.41}$$

Alternatively these particle/hole Hamiltonians can be written in terms of Pauli matrices, respectively: $\mathcal{H}_e = \xi_k\sigma_0 + B\sigma_2 + uk\sigma_3$ and $\mathcal{H}_h = -\xi_k\sigma_0 + B\sigma_2 + uk\sigma_3$. The eigenvalues E_k^e and E_k^h of $\mathcal{H}_e$ and $\mathcal{H}_h$ respectively are found using the Pauli algebra

$$E_{k\pm}^e = \xi_k \pm K \quad \text{and} \quad E_{k\pm}^h = -(\xi_k \pm K) \quad \text{where} \quad K := \sqrt{u^2k^2 + B^2}. \tag{2.42}$$

The corresponding eigenvectors can be found by writing the following conditions

$$\psi^e_{k\pm} = \begin{pmatrix} a_\pm \\ b_\pm \end{pmatrix} \quad \text{and} \quad \psi^h_{k\pm} = \begin{pmatrix} c_\pm \\ d_\pm \end{pmatrix} \quad \text{requiring} \quad \mathcal{H}_e\psi^e_{k\pm} = E^e_{k\pm}\psi^e_{k\pm} \quad \text{and} \quad \mathcal{H}_h\psi^h_{k\pm} = E^h_{k\pm}\psi^h_{k\pm}. \tag{2.43}$$

These conditions amount to the following relations

$$b_\pm = \frac{1}{iB}(\xi_k + uk - E_{k\pm})a_\pm = \frac{1}{iB}(uk \mp K)a_\pm \quad \text{and} \quad d_\pm = -\frac{iBc_\pm}{uk+K}, \tag{2.44}$$

which gives the following four eigenvectors: two for particles and two for holes respectively,

$$\psi^e_{k-} = \frac{1}{\mathcal{N}^e}\begin{pmatrix} iB \\ uk+K \end{pmatrix}, \quad \psi^e_{k+} = \frac{1}{\mathcal{N}^e}\begin{pmatrix} uk+K \\ iB \end{pmatrix}, \quad \psi^h_{k+} = \frac{1}{\mathcal{N}^h}\begin{pmatrix} uk-K \\ iB \end{pmatrix} \quad \text{and} \quad \psi^h_{k-} = \frac{1}{\mathcal{N}^h}\begin{pmatrix} iB \\ uk-K \end{pmatrix}. \tag{2.45}$$

The normalization factors are defined $\mathcal{N}^e := \sqrt{B^2 + (uk+K)^2}$ and $\mathcal{N}^h := \sqrt{B^2 + (uk-K)^2}$. The sign convention here is such that the $-$ solutions are low energy while the $+$ are high energy in both hole and particle blocks.

Now define a unitary transformation $\mathcal{U} := \mathcal{U}^e \oplus \mathcal{U}^h = \begin{pmatrix} \psi^e_{k-} & \psi^e_{k+} \end{pmatrix} \oplus \begin{pmatrix} \psi^h_{k+} & \psi^h_{k-} \end{pmatrix}$, that diagonalizes $\mathcal{K}$ in the following manner

$$\mathcal{U}^\dagger\mathcal{K}\mathcal{U} = \begin{pmatrix} E^e_{k-} & 0 & 0 & 0 \\ 0 & E^e_{k+} & 0 & 0 \\ 0 & 0 & E^h_{k+} & 0 \\ 0 & 0 & 0 & E^h_{k-} \end{pmatrix}. \tag{2.46}$$

The full model, assuming $B > 0$, under this unitary transformation yields

$$\mathcal{U}^\dagger\mathcal{H}\mathcal{U} = \left(\begin{array}{cc|cc} E^e_{k-} & 0 & \multicolumn{2}{c}{(U^e)^\dagger\Delta U^h} \\ 0 & E^e_{k+} & & \\ \hline \multicolumn{2}{c|}{(U^h)^\dagger\Delta^\dagger U^e} & E^h_{k+} & 0 \\ & & 0 & E^h_{k-} \end{array}\right) = \frac{1}{K}\left(\begin{array}{cc|cc} KE^e_{k-} & 0 & \delta B & -i\delta uk \\ 0 & KE^e_{k+} & i\delta uk & -\delta B \\ \hline \delta B & -i\delta uk & KE^h_{k+} & 0 \\ i\delta uk & -\delta B & 0 & KE^h_{k-} \end{array}\right). \tag{2.47}$$

The final part is to define the two complementary orthogonal projections[6]

$$P := \begin{pmatrix} 1 & 0 & 0 & 0 \\ 0 & 0 & 0 & 0 \\ 0 & 0 & 0 & 0 \\ 0 & 0 & 0 & 1 \end{pmatrix} \quad \text{and} \quad Q := 1 - P = \begin{pmatrix} 0 & 0 & 0 & 0 \\ 0 & 1 & 0 & 0 \\ 0 & 0 & 1 & 0 \\ 0 & 0 & 0 & 0 \end{pmatrix}. \tag{2.48}$$

Note that P projects to the low energy particle and holes. Using a so called *Schrieffer-Wolff* approximation scheme we may formulate an effective Hamiltonian for describing this system

$$\mathcal{H}_{\text{eff}}(k) = P\mathcal{U}^\dagger\mathcal{H}\mathcal{U}P + P\mathcal{H}_\delta Q(EQ - Q\mathcal{U}^\dagger\mathcal{H}\mathcal{U}Q)^{-1}Q\mathcal{H}_\delta P, \tag{2.49}$$

where $\mathcal{H}_\delta$ is just the block off-diagonal terms of eq. (2.47), such that $\mathcal{H} = \mathcal{K} + \mathcal{H}_\delta$. The inverse here only makes sense in the subspace of $Q\mathscr{H}$ [here $\mathscr{H}$ is the Fock space of each momentum k], i.e. 'in the central 2×2 block'. Assume $E \ll |E^{e(h)}_{k\pm}|$, then the inverse in the high energy $\begin{pmatrix} \psi^e_{k+} & \psi^h_{k+} \end{pmatrix}$ basis

$$(Q\mathcal{U}^\dagger\mathcal{H}\mathcal{U}Q)^{-1} = \left[-\frac{\delta uk}{K}\sigma_2 + E^e_{k+}\sigma_3\right]^{-1} = \left(\frac{\delta^2u^2k^2}{K^2} + (E^e_{k+})^2\right)^{-1}\left[-\frac{\delta uk}{K}\sigma_2 + E^e_{k+}\sigma_3\right]. \tag{2.50}$$

For simplicity define the place holder variable $z := \frac{\delta^2u^2k^2}{K^2} + (E^e_{k+})^2$. One then finds the effective Hamiltonian in the low energy basis $\begin{pmatrix} \psi^e_{k-} & \psi^h_{k-} \end{pmatrix}$ to be

$$\mathcal{H}_{\text{eff}}(k) = \frac{\delta(zK^2 + \delta^2B^2)uk}{zK^3}\sigma_2 + \frac{E^e_{k+}\delta^2B^2 + E^e_{k-}zK^2}{zK^2}\sigma_3. \tag{2.51}$$

If the gap is assumed to be comparatively small to $E^{e(h)}_{k\pm}$ and $uk \ll B$ we may set $z \approx (E^e_{k+})^2$ and $K \approx B$ such that the effective Hamiltonian reduces to the following effective p-wave superconducting Hamiltonian

$$H_{\text{eff}}(k) \approx \begin{pmatrix} \frac{k^2}{2m} - \mu - B + \frac{\delta^2}{B} & -i\frac{\delta u}{B}k \\ i\frac{\delta u}{B}k & -\frac{k^2}{2m} + \mu + B - \frac{\delta^2}{B} \end{pmatrix} = \begin{pmatrix} \frac{k}{2m} - \mu' & -i\Delta k \\ i\Delta k & -\frac{k}{2m} + \mu' \end{pmatrix} = \xi'_k\sigma_3 + \Delta k\sigma_2, \tag{2.52}$$

[6]There might be some interesting math here. These projections defined for each k on the momentum manifold are a collection of operators, projecting the spinors of the Fock space onto two orthogonal sub spaces consisting of the $+$ and $-$ solutions. $\mathscr{H} = \mathscr{H}_- \oplus \mathscr{H}_+$ as $\mathscr{H}_-^\perp = \mathscr{H}_+$ (suppressing k indexing).

where $\xi'_k := \frac{k^2}{2m} - \mu - B + \frac{\delta^2}{B}$ is the effective quasi-particle energies with a new chemical potential $\mu' := \mu + B - \frac{\delta^2}{B}$ and the gap parameter is $\Delta = \frac{\delta u}{B}$.

This is a profound result! In conclusion we have found that a one dimensional superconducting wire with spin-orbit interaction and subjected to a strong magnetic field can be described by a p-wave superconducting model. It has been proposed extensively that Majorana modes can exist in p-wave superconductors. For example one would expect to find these Majorana modes localized in the center of vortices in 2D systems or to be found near the ends of 1D wire structures, see e.g. [7].

2.4 Impurity Potentials in the Low Energy Model

Now we have an effective model for describing superconductivity induced in a semiconductor with spin-orbit interaction and subjected to a magnetic field which mimics a p-wave superconductor. The recurring theme is to ask ourselves what might be the effect of disorder found in the semiconductor? The answer will be the subject of this section. Physically there might be accidental impurities from the manufacturing process of semi-metals or they might be intentional as in doping, either giving or removing an electron locally. The effect of such impurities may or may not depend on the spin polarization of impurities and as such reflect this discrepancy. Furthermore we will consider only low densities of impurities so they may be effectively described by an array of delta functions as before.

The idea is to transform the impurity potential $\mathcal{Y}$ of eq. (2.19) into the low energy effective model from above. First the impurity potential must be rotated into the high/low energy basis

$$\begin{aligned}\mathcal{U}^\dagger \mathcal{Y} U = \frac{1}{K}&\begin{pmatrix} Kv_k - (Bw_{2,k} + ukw_{3,k}) & Kw_{1,k} + iukw_{2,k} - iBw_{3,k} \\ Kw_{1,k} - iukw_{2,k} + iBw_{3,k} & Kv_k + Bw_{2,k} + ukw_{3,k} \end{pmatrix} \\ &\oplus \begin{pmatrix} -Kv_k - (Bw_{2,k} - ukw_{3,k}) & -Kw_{1,k} + iukw_{2,k} + iBw_{3,k} \\ -Kw_{1,k} - iukw_{2,k} - iBw_{3,k} & -Kv_k + (Bw_{2,k} - ukw_{3,k}) \end{pmatrix}. \end{aligned} \tag{2.53}$$

Then projecting onto the low energy basis $\begin{pmatrix} \psi^e_{k-} & \psi^h_{k-} \end{pmatrix}$, with the projector P defined in eq. (2.48), gives

$$P\mathcal{U}^\dagger \mathcal{Y} \mathcal{U} P = \frac{1}{K}\begin{pmatrix} Kv_k - (Bw_{2,k} + ukw_{3,k}) & 0 \\ 0 & -Kv_k + (Bw_{2,k} - ukw_{3,k}) \end{pmatrix} = \frac{1}{K}\left[(Kv_k - Bw_{2,k})\sigma_3 - ukw_{3,k}\sigma_0\right]. \tag{2.54}$$

In the limit where $uk \ll B$ this reduces to

$$\mathcal{Y}_{\text{eff}} = P\mathcal{U}^\dagger \mathcal{Y} \mathcal{U} P \approx (v_k - w_{2,k})\sigma_3 - \frac{uk}{B} w_{3,k}\sigma_0. \tag{2.55}$$

Define the effective low energy versions of the spinless and spinful disorder potentials, respectively

$$\mathcal{V}_{\text{eff}} := v_k \sigma_3 \quad \text{and} \quad \mathcal{W}_{\text{eff}} := -w_{2,k}\sigma_3 - \frac{uk}{B} w_{3,k}\sigma_0, \tag{2.56}$$

here the potentials are not spinless and spinful but rather one of them is particle/hole symmetric and the other is not, respectively. In fact, already from the form presented here, the first term $w_{2,k}\sigma_3$ in $\mathcal{W}_{\text{eff}}$ looks remarkably similar to the spinless potential. Indeed as found below they are essentially the same in the bulk.

Finally note that the spinful disorder potential is not diagonalized by the unitary $\mathcal{U}$ and therefore enables transitions between high and low energy states. From eq. (2.53) we can qualitatively state that only the spinful impurity potential mixes the high and low energy states. The transition probabilities of going between high and low energies for electrons and holes calculated using Fermi's golden rule are respectively

$$\Gamma_{e_- \to e_+} \propto \left|\langle \psi^e_{k+} | \mathcal{U}^\dagger \mathcal{Y} \mathcal{U} | \psi^e_{k-} \rangle\right|^2 = \frac{1}{K^2}\left(K^2 |w_{1,k}|^2 + |ukw_{2,k} - Bw_{3,k}|^2\right), \quad \text{and} \tag{2.57}$$

$$\Gamma_{h_- \to h_+} \propto \left|\langle \psi^h_{k+} | \mathcal{U}^\dagger \mathcal{Y} \mathcal{U} | \psi^h_{k-} \rangle\right|^2 = \frac{1}{K^2}\left(K^2 |w_{1,k}|^2 + |ukw_{2,k} + Bw_{3,k}|^2\right). \tag{2.58}$$

However the states transitioned to must be of roughly equal energy for these to occur, as such they are modulated by the density of states of the final state.

2.5 SC1BA on the Effective p-wave Superconducting Model

The pieces of the puzzle have been put on the table and we are left to put it together. The topic of this section is to apply the self-consistent approximation on the effective p-wave model found previously–using the potentials projected onto this model. To be specific we apply the self-consistent First Born approximation scheme with

potentials as found in eq. (2.56) on the p-wave model of eq. (2.52). Proceeding in a similar fashion as with the 4x4 BCS above, the bare Green's function of the system (i.e. the clean system propagator) is now

$$\mathcal{G}_0^{-1}(k, i\omega_n) = i\omega_n\sigma_0 - \xi_k\sigma_3 - \Delta k\sigma_2. \tag{2.59}$$

Furthermore, parametrizing the impurity averaged Green's function $\mathcal{G}^{-1}$ in a similar fashion as before in terms of the renormalized parameters

$$\mathcal{G}^{-1}(k, i\omega_n) = i\tilde{\omega}_n\sigma_0 - \tilde{\xi}_k\sigma_3 - \tilde{\Delta}k\sigma_2. \tag{2.60}$$

Apriori assume the strength of the pairing is changed after renormalization, i.e. $\tilde{\Delta}(k) := \tilde{\Delta}k$ similar to the way the dispersion is renormalized $\tilde{\xi}_k = \frac{k^2}{2m^*} - \tilde{\mu}$.[7]

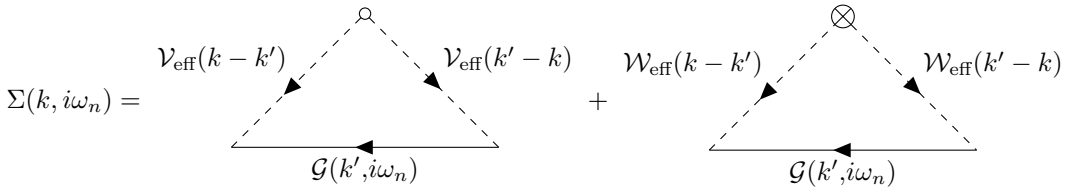

Figure 6: Feynman diagram scattering on the two effective types of impurities: spinless and spinful, represented by vertices $\circ$ and $\otimes$ respectively.

The self-energy of Fig. 6 here is of similar structure to that found in Fig. 1 and may be found using the Feynman rules to be

$$\begin{aligned}
\Sigma(k, i\omega_n) &= \frac{1}{L}\sum_{k'}(\mathcal{V}_{\text{eff}}(k-k')\mathcal{G}(k', i\omega_n)\mathcal{V}_{\text{eff}}(k'-k)) + \frac{1}{L}\sum_{k'}\langle(\mathcal{W}_{\text{eff}}(k-k')\mathcal{G}(k', i\omega_n)\mathcal{W}_{\text{eff}}(k'-k)\rangle_S \\
&= \frac{1}{L}\sum_{k'}|v_{k-k'}|^2\sigma_3\mathcal{G}(k', i\omega_n)\sigma_3 \qquad (2.61a) \\
&+ \frac{1}{L}\sum_{k'}\left\langle\left(w_{2,k-k'}\sigma_3 + \frac{u(k-k')}{B}w_{3,k-k'}\right)\mathcal{G}(k', i\omega_n)\left(w_{2,k'-k}\sigma_3 + \frac{u(k'-k)}{B}w_{3,k'-k}\right)\right\rangle_S. \qquad (2.61b)
\end{aligned}$$

The choice of inverse impurity averaged Green's Function in eq. (2.60) means $\mathcal{G}$ takes the form

$$\mathcal{G}(k, i\omega_n) = -\frac{i\tilde{\omega}_n + \tilde{\xi}_k\sigma_3 + \tilde{\Delta}k\sigma_2}{\tilde{\omega}_n^2 + \tilde{\xi}_k^2 + \tilde{\Delta}^2k^2}. \tag{2.62}$$

The first term in the self-energy, eq. line (2.61a), is already of a similar structure as that to the 4×4 model in eq. (2.23). In the second term, eq. line (2.61b), expressions like

$$\frac{u(k-k')}{B}w_{3,k-k'}\mathcal{G}(k', i\omega_n)\frac{u(k'-k)}{B}w_{3,k'-k} \propto \frac{u^2k^2}{B^2}, \tag{2.63}$$

are suppressed by the assumption $uk \ll B$ and can effectively be ignored. Furthermore the cross terms

$$w_{2,k-k'}\sigma_3\mathcal{G}(k', i\omega_n)\frac{u(k'-k)}{B}w_{3,k'-k} + \frac{u(k-k')}{B}w_{3,k-k'}\mathcal{G}(k', i\omega_n)w_{2,k'-k}\sigma_3 \propto S_{2,\beta}S_{3,\beta'}, \tag{2.64}$$

are identically zero after averaging over spins. Leaving only contribution from the term

$$w_{2,k-k'}\sigma_3\mathcal{G}(k', i\omega_n)w_{2,k'-k}\sigma_3 = |w_{2,k-k'}|^2\mathcal{G}(-k', i\omega_n). \tag{2.65}$$

This gives the self-energy in the SC1BA

$$\begin{aligned}
\Sigma(k, i\omega_n) &= \frac{1}{L}\sum_{k'}|v_{k-k'}|^2\sigma_3\mathcal{G}(k', i\omega_n)\sigma_3 + \frac{1}{L}\sum_{k'}\langle|w_{2,k-k'}|^2\sigma_3\mathcal{G}(k', i\omega_n)\sigma_3\rangle_S \\
&= N_i|V|^2\frac{1}{L}\sum_{k'}\sigma_3\mathcal{G}(k', i\omega_n)\sigma_3 + \frac{1}{3}S(S+1)N_\beta\frac{1}{L}\sum_{k'}\sigma_3\mathcal{G}(k', i\omega_n)\sigma_3.
\end{aligned} \tag{2.66}$$

[7] Note that any the coefficient of any non-constant polynomial in k cannot be changed under the SC1BA with delta-like disorder. These coefficients, such as $1/2m$ and Δ contribute in renormalizing the terms constant in k, i.e. the coefficients of the k^0 terms.

The factor 1/3 comes from the spin average by replacing S_y with $S/3$ and similar to the 4×4 case of the BCS model define:

$$\tau_i^{-1} := N_i|V|^2 \quad \text{and} \quad \tau_\beta^{-1} := \frac{1}{3}S(S+1)N_\beta|W|^2. \tag{2.67}$$

Using the standard parametrization of the Green's function in eq. (2.60) we can use the general formalism described in Appendix B to calculate the sums in the self-energy and find

$$\frac{1}{L}\sum_k \mathcal{G}(k, i\omega_n) = -\tilde{f}_n \left[i\tilde{\omega}_n + \tilde{g}_n\sigma_3\right], \tag{2.68}$$

which define the place holder functions $\tilde{f}_n$ and $\tilde{g}_n$. These vary in a not necessarily continuous manner depending on the parameter regime we are working in. Similarly to above there is one parameter regime which dominate the others, in this case the functions

$$\tilde{f}_n := \frac{i}{8mS_+S_-\sqrt{m^2\tilde{\Delta}^4 - 2m\tilde{\mu}\tilde{\Delta}^2 - \tilde{\omega}_n^2}} \quad \text{and} \quad \tilde{g}_n := (R_+ - \tilde{\mu})S_-^1 + (R_- - \tilde{\mu})S_+^1. \tag{2.69}$$

Here $S_\pm$ are the roots in k-space of the denominator of $\mathcal{G}$ in eq. (2.62) and $R_\pm$ are the energy roots of $\epsilon = \frac{k^2}{2m}$,

$$S_\pm = \sqrt{2m}\sqrt{(\tilde{\mu} - m\tilde{\Delta}^2) \pm \sqrt{m^2\tilde{\Delta}^4 - 2m\tilde{\mu}\tilde{\Delta}^2 - \tilde{\omega}_n^2}}. \tag{2.70}$$

From the algebraic equation for the self-energy, $\Sigma = \mathcal{G}_0^{-1} - \mathcal{G}^{-1}$, combined with the expression from SC1BA the self-consistent equation reads

$$\begin{aligned}(i\omega_n - i\tilde{\omega}_n) - (\xi_k - \tilde{\xi}_k)\tau_3 - (\Delta(k) - \tilde{\Delta}(k))\sigma_2 &= \frac{1}{\tau_i}\sum_{k'}\sigma_3\mathcal{G}(k', i\omega_n)\sigma_3 + \frac{1}{\tau_\beta}\sum_{k'}\sigma_3\mathcal{G}(k', i\omega_n)\sigma_3 \\ &= -\left(\frac{1}{\tau_i} + \frac{1}{\tau_\beta}\right)\tilde{f}_n\left[i\tilde{\omega}_n + \tilde{g}_n\sigma_3\right].\end{aligned} \tag{2.71}$$

Breaking this down component wise self-consistent equations for each parameter are found

$$i\tilde{\omega}_n = i\omega_n + \tilde{f}_n\left[\frac{1}{\tau_i} + \frac{1}{\tau_\beta}\right]i\tilde{\omega}_n, \quad \tilde{\mu} = \mu + \tilde{f}_n\tilde{g}_n\left[\frac{1}{\tau_i} + \frac{1}{\tau_\beta}\right] \quad \text{and} \quad \tilde{\Delta} = \Delta. \tag{2.72}$$

It is noteworthy that the superconducting gap parameter Δ is not changed by the renormalization process and likewise is the mass m unchanged. The other parameters of the system change however and these equations are even more complicated than the self-consistent equations from Rickayzen [10], eq. (2.29), or even the exact solutions found for the s-wave SC in eq. (2.38). Furthermore, the parameters τ_i^{-1} and τ_β^{-1} occur in the self-consistent equations only as the sum of the two. From this we can infer the p-wave superconducting state is effected equivalently by both types of impurities τ_i^{-1} and τ_β^{-1}. By comparison remember that the s-wave superconductor was entirely unphased by non-magnetic type impurities.

The density of states for the p-wave superconductor can be expressed using the impurity averaged Green's function

$$d_s(\omega) = \lim_{\eta\to 0}\mathrm{Im}[\mathcal{G}(0,0,\omega + i\eta)] = \lim_{\eta\to 0}\mathrm{Im}[\tilde{f}(\tilde{\omega})(\tilde{\omega}\tilde{h}(\tilde{\omega}) + \tilde{g}(\tilde{\omega})\tau_3)]. \tag{2.73}$$

Formulated in this manner it is very similar to the s-wave superconductor, however as we know the functions f, h and g are different. The DOS for the p-wave superconductor is plotted in Fig. 7 below.

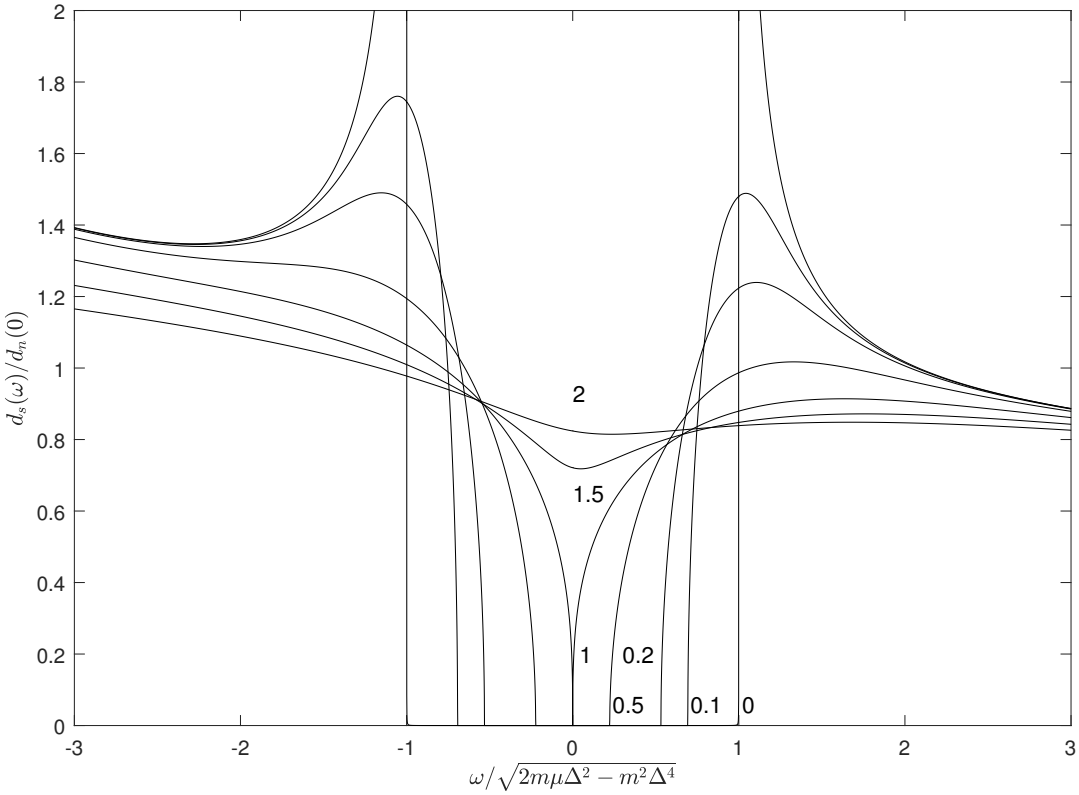

Figure 7: Plot of the normalized density of states for a p-wave superconductor system with different disorder strengths. The disorder strength τ_β^{-1} or τ_i^{-1} goes from 0 to 2 as indicated near the graphs and the relation between the gap and chemical potential is $\mu/\Delta = 10^2$. See main text for a more detailed description.

Despite the fundamental difference between the s-wave and p-wave superconductors in our model, the density of states appears remarkably similar–compare Figs. 4 and 7. The frequencies have been rescaled by $\sqrt{2m\mu\Delta^2 - m^2\Delta^4}$ as this is the point of the singularities nearest zero in the DOS in the function f_n from eq. (2.69). So the gap in the superconducting density of states without impurities is $2\sqrt{2m\mu\Delta^2 - m^2\Delta^4}$ rather than the usual 2Δ from BCS theory. The effect of added impurities is to broadening these coherence peaks and the eventual closing of the superconducting gap.

The p-wave superconductor is affected equivalently by the magnetic and non-magnetic impurities τ_β^{-1} and τ_i^{-1}, furthermore the hard gap closes completely at $\tau_i^{-1} + \tau_\beta^{-1} \approx 8m^2\Delta\mu$. It is clear from eq. (2.72) that this should in fact be additive. This characteristic disorder strength was found by varying the parameters of the system independently and codependently to find a numerical value of $8m^2\Delta\mu$. Interestingly this characteristic disorder strength is proportional to μ rather than $\sqrt{\mu}$ as was the case for the s-wave superconductor. Both for p-wave and s-wave this disorder strength is directly proportional to the gap parameter Δ.

The p-wave DOS appears to be much more sensitive to the relation μ/Δ, but this is attributed to the rescaled axis on Fig. 7 as the gap in the DOS is significantly larger for the p-wave than the s-wave SC when the chemical potential is large. For a comparatively small chemical potential $\mu = 30$ see Fig. 8 below. Notice how the Van Hove peak is broadened by increasing the impurity strength τ_β^{-1} or τ_i^{-1}, that is the Van Hove peak is also affected by both magnetic and non-magnetic impurities as expected.

Note also that there is no phantom peak in Fig. 8 contrary to what was found for the s-wave superconductor. This might suggest the phantom peak to really be a numerical error.

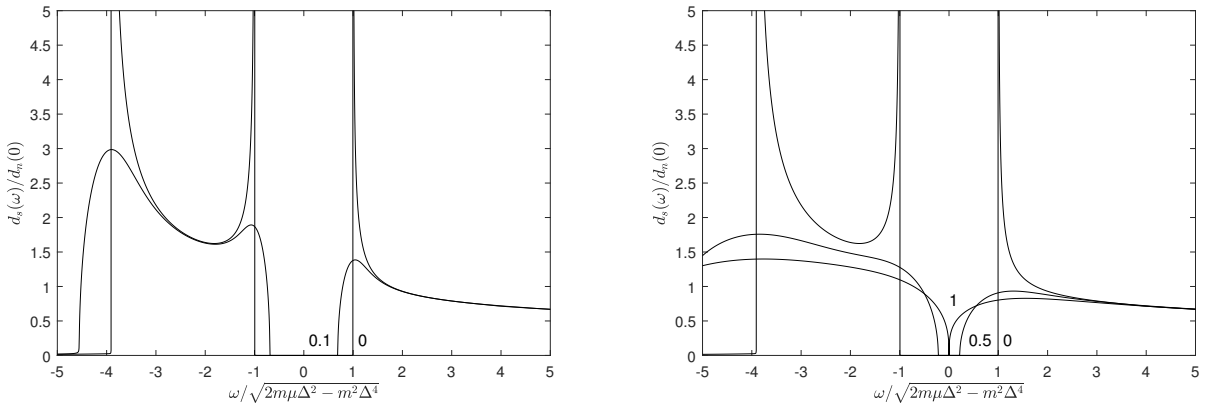

(a) Effect of weak disorder on the DOS.

(b) Effect of strong disorder on the DOS.

Figure 8: DOS at different impurities at a low filling $\mu/\Delta = 3 \cdot 10^1$. A broadening of the frequency ω was imposed as $i\eta = i10^{-4}$. Fig. (a): the disorder strength τ_β^{-1} goes from 0 to 0.1. Fig. (b): the disorder strength τ_β^{-1} goes from 0 to 1.5. See the main text for more detail.

So far we have categorized the effects of the disorder on the non-local DOS in the p-wave superconductor for small μ. The next target is pushing the limit of extremely low filling $\mu \to 0$. Naively we could imagine the effect of taking this limit to be represented by moving the Van Hove singularity towards the coherence peaks. However by inspection the singularities become imaginary for μ smaller than the critical value of $\mu_c = \frac{1}{2}m\Delta^2$. Below this value the coherence peaks are broadened by decreasing μ in a similar fashion to how the impurities would effect them as seen in Fig. 8. This effect is demonstrated in Fig. 9 below at $\tau_\beta^{-1} = \tau_i^{-1} = 0$. For all values of μ at or below μ_c there is a gap in the DOS of width 2μ, however the coherence peaks are gone. Instead there is a single peak at $\omega = \mu$ which decays at a rate of $\omega^{-1/2}$. Instead of a peak at $\omega/\mu = 1$ there is a soft bump $\omega/\mu = 2$ for $\mu = \mu_c$ which is further broadened and shifted to the right as μ is decreased.

Particularly for no impurities, $\tau_\beta^{-1} = \tau_i^{-1} = 0$, as μ approaches μ_c from above the Van Hoven peak moves closer to the coherence peak at $\omega = -\sqrt{2m\mu\Delta^2 - m^2\Delta^4}$. As μ is lowered the otherwise vanishing DOS to the left of $-\mu$ is continuously transformed into a tail decaying as $\omega^{-1/2}$ when μ reaches μ_c as shown in Fig. 9 (a).

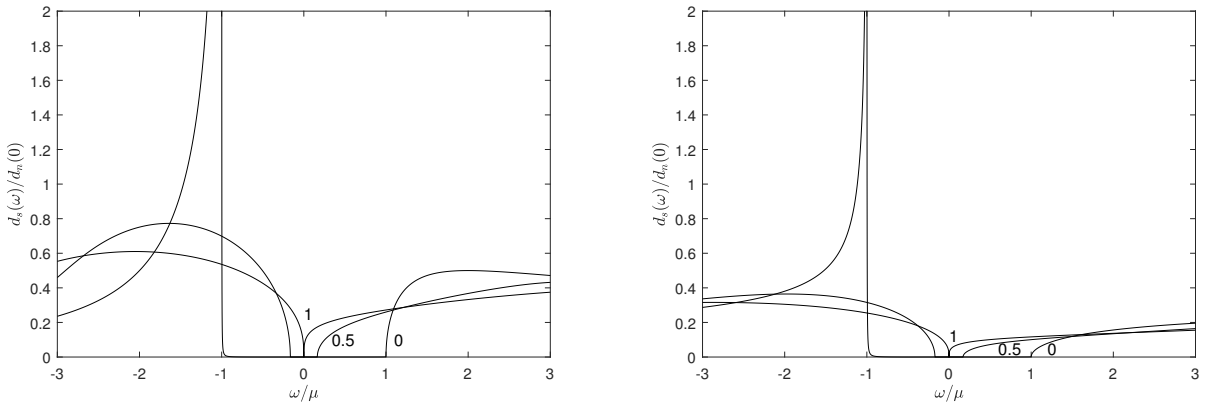

(a) Effect of impurities on the DOS at $\mu = \mu_c$.

(b) Effect of impurities on the DOS at μ below μ_c.

Figure 9: DOS at different impurities at a two very low fillings. A broadening of the frequency ω was imposed as $i\eta = i10^{-4}$. See the main text for more detail. The disorder strength τ_β^{-1} goes from 0 to 1 on both figures and the chemical potential is changed between them. Fig. (a): the chemical potential is tuned at a value $\mu = \frac{1}{2}m\Delta^2$. Fig. (b): the chemical potential is tuned to $\mu = 0.1m\Delta^2$.

In Fig. 9 the changing behavior of the density of states for different impurity strengths is plotted. Astonishingly the influence of impurities is similar to that of μ greater than μ_c! The effect of τ_β^{-1} is equivalent to that of τ_i^{-1} and the gap closes for the same critical value of $\tau_i^{-1} + \tau_\beta^{-1} \approx 8m^2\Delta\mu$.

3 Local Green's Functions and Disorder in the Semi-Infinite TS Wire

Of particular interest is the ends of a topological superconducting [TS] wire since here the Majorana Fermions should reside. As such, a thorough investigation of the end of the wire is required. Previously we have dealt only with the bulk of the wire and must modify the model slightly to realize such an investigation. As has been studied, e.g. by Zazunov et. al. [14] or Alvarado et. al. [1], this can be realized through a model for a semi-infinite TS wire, e.g. going from $x = 0$ to $x = \infty$. One method of realizing this semi-infinite wire is to introduce a scattering potential at $x = 0$ in the existing infinite TS wire. This effectively cuts the wire in half and as we let the strength of this scattering potential grow we will obtain two non-interacting distinct semi-infinite wires.

To be precise, introduce the potential $\mathcal{U}(x) = U\delta(x)\sigma_3$ with characteristic strength U. The Dyson equation for this system with the scattering potential is then

$$\bar{\mathcal{G}}(x,x') = \mathcal{G}_0(x,x') + \int_{\mathbb{R}} \mathcal{G}_0(x,y)\mathcal{U}(y)\bar{\mathcal{G}}(y,x')\,\mathrm{d}y = \mathcal{G}_0(x,x') + \mathcal{G}_0(x,0)U\sigma_3\bar{\mathcal{G}}(0,x'). \tag{3.1}$$

Using this equation we may first obtain an equation for $\bar{\mathcal{G}}(0,x')$ and then put it back into eq. (3.1) to find $\bar{\mathcal{G}}(x,x')$. First for $\bar{\mathcal{G}}(0,x')$

$$\bar{\mathcal{G}}(0,x') = [1 - \mathcal{G}_0(0,0)U\sigma_3]^{-1}\mathcal{G}_0(0,x'). \tag{3.2}$$

Putting this back into the Dyson equation of eq. (3.1) a solution for $\bar{\mathcal{G}}$ is found

$$\bar{\mathcal{G}}(x,x') = \mathcal{G}_0(x,x') + \mathcal{G}_0(x,0)[U^{-1}\sigma_3 - \mathcal{G}_0(0,0)]^{-1}\mathcal{G}_0(0,x'). \tag{3.3}$$

Taking the limit as $U \to \infty$ yields the TS wire Green's function of interest

$$\bar{\mathcal{G}}(x,x') = \mathcal{G}_0(x,x') - \mathcal{G}_0(x,0)\mathcal{G}_0^{-1}(0,0)\mathcal{G}_0(0,x'). \tag{3.4}$$

Although the Green's function for the infinite TS wire $\mathcal{G}_0$ has a nice diagonal form in k-space this is untrue for the semi-infinite wire described by $\bar{\mathcal{G}}$. Therefore we keep things in real space for the time being.

3.1 SC1BA on a semi-finite TS wire

We remind ourselves the motivation is to find Majorana modes at the end of the TS wire. These will in fact appear as zero-bias peaks in the density of states of $\bar{\mathcal{G}}$ near the ends of the wire, that is not exactly $x = 0$ but close enough as the Majorana mode will decay exponentially as $e^{-x/\xi}$ in the wire, here ξ is the localization length. But we again ask ourselves what happens when there are impurities present in the wire. This question will be answered with the Born approximation.

So to apply the SC1BA to the semi-infinite wire we first need to restate the theory in real space coordinates. The Dyson equation for the impurity averaged Green's function $\mathcal{G}$ in real space is

$$\mathcal{G}(x,x') = \bar{\mathcal{G}}(x,x') + \int \bar{\mathcal{G}}(x,y)\mathcal{V}(y)\mathcal{G}(y,x')\,\mathrm{d}y\,. \tag{3.5}$$

Notice here $\bar{\mathcal{G}}$ is the bare Green's function of the system, that is the semi-infinite wire–without impurities. Using the recursive nature of this equation we may define the self-energy Σ by inserting $\mathcal{G}$ in the right hand side repeatedly

$$\mathcal{G}(x,x') = \bar{\mathcal{G}}(x,x') + \iint \bar{\mathcal{G}}(x,y)\Sigma(y,z)\bar{\mathcal{G}}(z,x')\,\mathrm{d}y\,\mathrm{d}z\,. \tag{3.6}$$

In this way of writing, the self-energy Σ is an infinite series of Green's functions and potentials. Particularly in the first Born approximation the self-energy is defined by

$$\Sigma(y,z) = \mathcal{V}(y)\bar{\mathcal{G}}(y,z)\mathcal{V}(z), \tag{3.7}$$

which means in the First Born approximation we can express the impurity averaged Green's function $\mathcal{G}$ as

$$\mathcal{G}(x,x') = \bar{\mathcal{G}}(x,x') + \iint \bar{\mathcal{G}}(x,y)\mathcal{V}(y)\bar{\mathcal{G}}(y,z)\mathcal{V}(z)\bar{\mathcal{G}}(z,x')\,\mathrm{d}y\,\mathrm{d}z\,. \tag{3.8}$$

We then wish to find an expression for the Green's function of the semi-infinite wire $\mathcal{G}$. First we write the position dependent parts of the inifinite wire Green's function

$$\mathcal{G}_0(x,0) = \int \mathcal{G}(k)e^{ikx}\,\mathrm{d}k\,, \quad \mathcal{G}_0(0,x') = \int \mathcal{G}(k)e^{-ikx'}\,\mathrm{d}k \quad \text{and} \quad \mathcal{G}_0(x,x') = \int \mathcal{G}(k)e^{ik(x-x')}\,\mathrm{d}k\,, \tag{3.9}$$

where from Appendix B we can parametrize $\mathcal{G}_0(x,x',i\omega_n)$ in terms of the functions f,g,h and j as

$$\mathcal{G}_0(x,x',i\omega_n) = -f_n\left[i\omega_n h_n(x-x') + g_n(x-x')\sigma_3 + i\Delta_0 j_n(x-x')\sigma_2\right]. \tag{3.10}$$

Inserting this expression for $\mathcal{G}_0$ into eq. (3.4) gives

$$\bar{\mathcal{G}}(x,x') = \mathcal{G}_0(x,x') - \mathcal{G}_0(x,0)\mathcal{G}_0^{-1}(0,0)\mathcal{G}_0(0,x') = i\Gamma_n(x,x')\sigma_0 + \Phi_n(x,x')\sigma_1 + \Psi_n(x,x')\sigma_2 + \chi_n(x,x')\sigma_3. \tag{3.11}$$

Where the non translation invariant functions Γ_n, Φ_n, Ψ_n and χ_n are defined as

$$\begin{aligned} i\Gamma_n(x,x') = {} & -i\omega_n f_n h_n(x-x') + i\omega_n \frac{f_n}{D_n}\big[h_n(x)(-\omega_n^2 h_n(-x')h_n(0) - g_n(-x')g_n(0)) - h_n(-x')g_n(x)g_n(0) \\ & - h_n(0)(\Delta^2 j_n(x)j_n(-x') - g_n(x)g_n(-x'))\big], \end{aligned} \tag{3.12a}$$

$$\Phi_n(x,x') = i\omega_n\Delta\frac{f_n}{D_n}\big[j_n(-x')(g_n(x)h_n(0) - h_n(x)g_n(0)) - g_n(-x')j_n(x)h_n(0) + h_n(-x')j_n(x)g_n(0)\big], \tag{3.12b}$$

$$\begin{aligned} \Psi_n(x,x') = {} & -i\Delta f_n j_n(x-x') - i\Delta\frac{f_n}{D_n}\big[j_n(x)(\omega_n^2 h_n(-x')h_n(0) + g_n(-x')g_n(0)) \\ & + j_n(-x')(\omega_n^2 h_n(x)h_n(0) + g_n(x)g_n(0))\big], \end{aligned} \tag{3.12c}$$

$$\begin{aligned} \chi_n(x,x') = {} & -f_n g_n(x-x') + \frac{f_n}{D_n}\big[-\omega_n^2 g_n(x)h_n(-x')h_n(0) + g_n(-x')(-\omega_n^2 h_n(x)h_n(0) - g_n(x)g_n(0)) \\ & + g_n(0)(\omega_n^2 h_n(x)h_n(-x') - \Delta^2 j_n(x)j_n(-x'))\big], \end{aligned} \tag{3.12d}$$

where the determinant $D_n = -\omega_n^2 h(0)^2 - g(0)^2$. To obtain these equations we have consistently set $j_0 = 0$ as dictated in Appendix B. It is important to note these equations go to zero when $x = x' = 0$ as we would expect from eq. (3.4).

We expect the self-energy to be diagonal in real space, i.e. $\Sigma(x,y) = \Sigma(x)\delta(x-y)$. These conditions may be derived from the imposed conditions

$$\langle\mathcal{V}(x)\mathcal{V}(x')\rangle_{\text{imp}} = \tau_i^{-1}\delta(x-x') \quad \text{and} \quad \langle\mathcal{W}(x)\mathcal{W}(x')\rangle_{\text{imp}} = \tau_\beta^{-1}\delta(x-x'). \tag{3.13}$$

These are really no different than the conditions imposed in previous sections. The full Green's function takes the form

$$\mathcal{G}(x,x') = \bar{\mathcal{G}}(x,x') + \iint \bar{\mathcal{G}}(x,y)\Sigma(y,y)\delta(y-z)\mathcal{G}(z,x')\,\mathrm{d}y\,\mathrm{d}z\,. \tag{3.14}$$

As found above we can insert the definition of $\bar{\mathcal{G}}$ and find the Dyson equation for $\mathcal{G}$ in terms of $\mathcal{G}_0$

$$\begin{aligned} \mathcal{G}(x,x') = {} & \mathcal{G}_0(x,x') - \mathcal{G}_0(x,0)\mathcal{G}_0^{-1}(0,0)\mathcal{G}_0(0,x') \\ & + \int\left[\mathcal{G}_0(x,y) - \mathcal{G}_0(x,0)\mathcal{G}_0^{-1}(0,0)\mathcal{G}_0(0,y)\right]\Sigma(y)\mathcal{G}(y,x')\,\mathrm{d}y \end{aligned} \tag{3.15}$$

However, this problem is immensely more complicated to solve compared to the infinite wire, as the inverse Green's Function is defined by the equation

$$\int \mathcal{G}^{-1}(x,y)\mathcal{G}(y,x')\,\mathrm{d}y = \delta(x-x'). \tag{3.16}$$

Because the Dyson equation is not algebraic this equation is solved by solving an integral equation–while minding the matrix algebra of the Green's functions.

One way to circumvent this is by considering the first Born approximation rather than its self-consistent counterpart. The full Green's function in the first Born approximation is stated above in eq. (3.8). From eq. (3.13) the self-energy is

$$\Sigma(x,x') = \frac{1}{\tau_i}(\sigma_3\bar{\mathcal{G}}(x,x')\sigma_3) + \frac{1}{\tau_\beta}(\sigma_3\bar{\mathcal{G}}(x,x')\sigma_3). \tag{3.17}$$

The p-wave superconductor is affected equally by both magnetic and non-magnetic impurities so we may put these together in a single impurity parameter $\tau^{-1} := \tau_\beta^{-1} + \tau_\beta^{-1}$. The expression for $\bar{\mathcal{G}}$ from eq. (3.14) with the self-energy expressed in the first Born approximation is

$$\mathcal{G}(x,x') = \bar{\mathcal{G}}(x,x') + \frac{1}{\tau}\int \bar{\mathcal{G}}(x,y)(\sigma_3\bar{\mathcal{G}}(y,y)\sigma_3)\bar{\mathcal{G}}(y,x')\,\mathrm{d}y\,. \tag{3.18}$$

The task is then to find this though numerical calculations.

Using the model for the semi-infinite wire we can calculate the non-local density of states. This is simply the imaginary part of $\bar{\mathcal{G}}$

$$d_s(x, x'; \omega) = -2\mathrm{Im}[\bar{\mathcal{G}}(x, x', \omega)]. \tag{3.19}$$

One such example is plotted in Fig. 10 below.

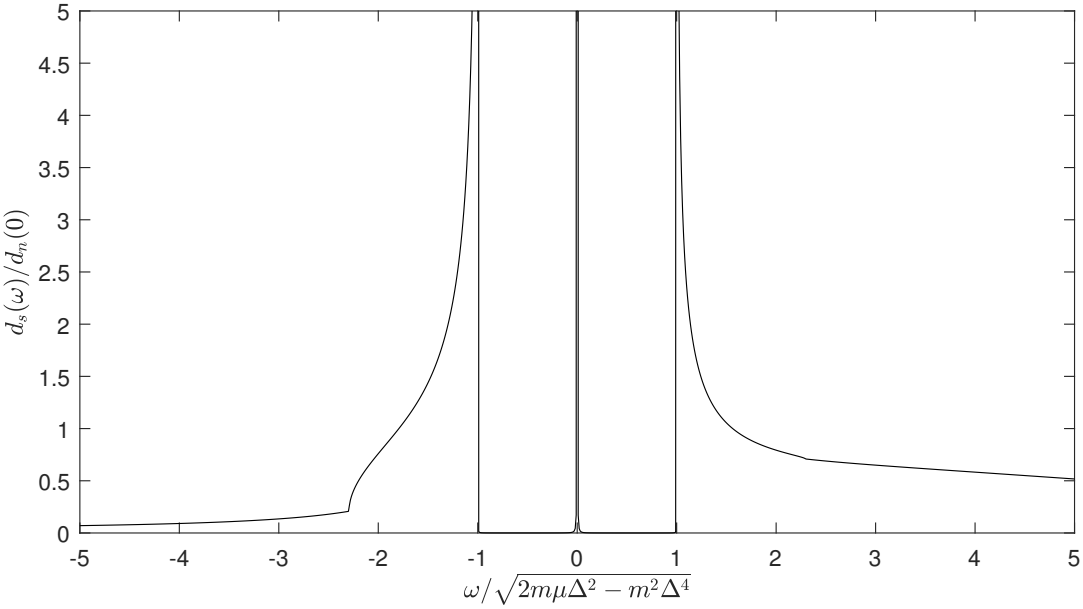

Figure 10: Position dependent DOS at $x = x' = 3\xi/100$ where ξ is the superconducting coherence length. The frequencies ω are broadened by $i\eta = i10^{-4}$.

In Fig. 10 the position dependent density of states for the semi-infinite TS wire is plotted. Notice the zero-bias peak signifying the presence of a zero energy Majorana state! The usual structure of the coherence peaks at $\omega = \pm\sqrt{2m\mu\Delta^2 - m^2\Delta^4}$ is also present. Note the figure is based on numerical simulation which do not produce the expected bulk DOS as x and x' is increased and we attribute this to numerical error–but it does verify $d_s(0, 0, \omega) = 0$ for all ω. Because of temporal restrictions we do not present results applying the Born approximation as described above. However we may still discuss and speculate on how the impurities would change the DOS shown in Fig. 10.

The overarching narrative in this thesis and particularly Chapters 2.2, 2.5 is that the self-consistent first Born approximation renormalizes the system parameters which broadens the singularities of the DOS. So a natural conclusion would be that this same effect would happen to the position dependent density of states in Fig. 10. That is, we expect the zero-bias peak and also the coherence peaks to be broadened as the impurity strength τ^{-1} is increased. We predict the peaks to be broadened so much for strong disorder that they are indistinguishable from the normal state density of states in the bulk.

This prediction is in stark contrast to the results found by Hui et. al. in [5]. They find that even for strong disorder, long after the coherence peaks are flattened out, that the zero-bias peak remains. Their approximation is similar to ours using a self-consistent (first) Born approximation, but with a linearized dispersion $\xi_k \approx v_F k$. Another point of differing methodology is their use of the Eilenberger Green's function rather than the Nambu Gorkov Green's function used in this thesis. One possible way of continuing this work is then to compare how this the SC1BA with the Nambu Gorkov Green's function differs from the SC1BA within Eilenberger theory.

Another subject of interest include considering how the Majorana modes are delocalized with increasing disorder. In fact, the localization length of the Majorana mode is predicted by Hui, in [5], to increase with disorder strength.

4 Conclusions

In this thesis we set out to consider the effects of disorder in superconducting systems. We did so through exact analytic calculations of the self-consistent first Born approximation [SC1BA] supplemented by numeric solutions to these self-consistent equations. First we applied SC1BA to the BCS theory of superconductivity and considered disorder effects in this simple system. Our main result is finding and analyzing an effective p-wave model that arises from superconducting systems with spin-orbit interactions and Zeeman splitting. This analysis consisted of deriving self-consistent equations and solving these numerically at non-zero disorder.

For the BCS superconductor the Born approximation prediction is in agreement with Anderson's theorem and is unphased by non-magnetic type disorder. For magnetic type impurities the characteristic BCS gap is closed in proportion to the disorder strength. Particularly, from numerical analysis, at a disorder strength close to $\Delta\sqrt{8m^3\mu}$ the gap closes completely.

We found a p-wave superconductor describes the low energy block of a BCS superconductor with spin orbit interaction and strong magnetic fields. Analyzing the p-wave superconductor with the Born approximation we find analytic equations implying the system to be sensitive to both magnetic as well as non-magnetic type disorder. This is verified by numerical simulations and in terms of the phenomenological disorder strengths the density of states is indeed found to be affected in equal proportions to both types of disorder. The coherence peaks of the p-wave gap are broadened by increasing the impurity densities and closes completely when the disorder strength is near $8m^2\Delta\mu$, which is found by numerical analysis.

A thorough analysis of the low filing limit for the topological superconducting wire was executed. We found interesting interplay between the Van Hoven and coherence peaks in this limit. At these low fillings the system is very sensitive to disorder.

Finally a semi-infinite wire is considered as a representation of a topological superconducting wire with a Majorana edge mode. We find analytic equations for describing such a system and simulate these numerically finding a zero-bias peak [ZBP] near the end of the wire. We propose the Born approximation in this semi-infinite wire could retain the ZBP for low disorder densities but expect it to disappear completely for strong disorder.

References

[1] M. Alvarado, A. Iks, A. Zazunov, R. Egger, and A. Levy Yeyati. Boundary green's function approach for spinful single-channel and multichannel majorana nanowires. *Physical Review B*, 101(9), Mar 2020.

[2] Sergey Bravyi, David P. DiVincenzo, and Daniel Loss. Schrieffer–wolff transformation for quantum many-body systems. *Annals of Physics*, 326(10):2793–2826, Oct 2011.

[3] Henrik Bruus and Karsten Flensberg. *Many-body quantum field theory in condensed matter physics: an introduction*. Oxford University Press, United Kingdom, 2016.

[4] Franti šek Herman and Richard Hlubina. Microscopic interpretation of the dynes formula for the tunneling density of states. *Phys. Rev. B*, 94:144508, Oct 2016.

[5] Hoi-Yin Hui, Jay D. Sau, and S. Das Sarma. Generalized eilenberger theory for majorana zero-mode-carrying disorderedp-wave superconductors. *Physical Review B*, 90(6), Aug 2014.

[6] Torsten Karzig, Christina Knapp, Roman M. Lutchyn, Parsa Bonderson, Matthew B. Hastings, Chetan Nayak, Jason Alicea, Karsten Flensberg, Stephan Plugge, Yuval Oreg, and et al. Scalable designs for quasiparticle-poisoning-protected topological quantum computation with majorana zero modes. *Physical Review B*, 95(23), Jun 2017.

[7] Martin Leijnse and Karsten Flensberg. Introduction to topological superconductivity and majorana fermions. *Semiconductor Science and Technology*, 27(12):124003, Nov 2012.

[8] Roman M. Lutchyn, Tudor D. Stanescu, and S. Das Sarma. Momentum relaxation in a semiconductor proximity-coupled to a disordereds-wave superconductor: Effect of scattering on topological superconductivity. *Physical Review B*, 85(14), Apr 2012.

[9] Yuval Oreg, Gil Refael, and Felix von Oppen. Helical liquids and majorana bound states in quantum wires. *Physical Review Letters*, 105(17), Oct 2010.

[10] G Rickayzen. *Theory of Superconductivity*. Interscience Publishers, New York, 1965.

[11] Jay D. Sau, Sumanta Tewari, and S. Das Sarma. Experimental and materials considerations for the topological superconducting state in electron- and hole-doped semiconductors: Searching for non-abelian majorana modes in 1d nanowires and 2d heterostructures. *Physical Review B*, 85(6), Feb 2012.

[12] René L. Schilling. *Measures, Integrals and Martingales*. Cambridge University Press, 2017.

[13] C. Tutschku, R. W. Reinthaler, C. Lei, A. H. MacDonald, and E. M. Hankiewicz. Majorana-based quantum computing in nanowire devices. *Physical Review B*, 102(12), Sep 2020.

[14] A. Zazunov, R. Egger, and A. Levy Yeyati. Low-energy theory of transport in majorana wire junctions. *Physical Review B*, 94(1), Jul 2016.

A Fourier Transformation Convention

The Fourier transformation is often useful to us as a manner of reducing the mathematical complexity of a physical problem. In this chapter we shall explore some formalism and establish our convention for this transformation as used throughout this thesis. I shall do this somewhat loosely, targeted towards physicists rather than use mathematical rigor. However I recommend looking into Chapter 19 in [12] for a more complete coverage of this subject.

In general we may assume a function f to be Lebesgue integrable on some finite region, e.g some hyper box $[\mathbf{0}, \mathbf{L}]$, i.e. $f \in \mathcal{L}^1_{\mathbb{C}}([\mathbf{0}, \mathbf{L}], \lambda)$ and $f \in \mathcal{L}^2_{\mathbb{C}}([\mathbf{0}, \mathbf{L}], \lambda)$. The Fourier transformation of f defined in a finite region is

$$f(\mathbf{r}) = \frac{1}{V} \sum_k f_{\mathbf{k}} e^{i\mathbf{k}\cdot\mathbf{r}} \quad \text{where} \quad k_i = \frac{2\pi n_i}{L_i}, \quad n_i \in \mathbb{Z}, \quad \forall i = 1, \ldots, d, \quad \text{and} \quad f_{\mathbf{k}} = \int_V f(\mathbf{r}) e^{-i\mathbf{k}\cdot\mathbf{r}} \, \mathrm{d}\mathbf{r} \,. \tag{A1}$$

where V is the hypervolume of the hyperbox. Importantly we have the following relations for the delta functions

$$\int e^{-i\mathbf{k}\cdot\mathbf{r}} \, \mathrm{d}\mathbf{r} = V \delta_{\mathbf{k}\mathbf{0}} \quad \text{and} \quad \frac{1}{V} \sum_{\mathbf{k}} e^{i\mathbf{k}\cdot\mathbf{r}} = \delta(\mathbf{r}). \tag{A2}$$

Taking the limit of $V \to \infty$ where the box region is very large we may consider all the reals as the domain and therefore define the Fourier transforms in the continuum as

$$f(\mathbf{r}) = \int_{\mathbb{R}^d} f(\mathbf{k}) e^{i\mathbf{k}\cdot\mathbf{r}} \frac{\mathrm{d}\mathbf{k}}{(2\pi)^d} \quad \text{and} \quad f(\mathbf{k}) = \int_{\mathbb{R}^d} f(\mathbf{r}) e^{-i\mathbf{k}\cdot\mathbf{r}} \, \mathrm{d}\mathbf{r} \,. \tag{A3}$$

We have the following important theorem.

Theorem A.1. *The Fourier Transformation of an odd(even) function is odd(even).*

Proof. The proof is a simple calculation, let $f : \mathbb{R}^d \to \mathbb{R}$ and denote by $\hat{f}$ its Fourier transform. Assume first f is odd, then by Jacobis transformation theorem

$$\hat{f}(\mathbf{k}) = \int_{\mathbb{R}^d} f(\mathbf{r}) e^{-i\mathbf{k}\cdot\mathbf{r}} \, \mathrm{d}\mathbf{r} = \int_{\mathbb{R}^d} f(-\mathbf{r}) e^{i\mathbf{k}\cdot\mathbf{r}} \, \mathrm{d}\mathbf{r} = -\int_{\mathbb{R}^d} f(\mathbf{r}) e^{i\mathbf{k}\cdot\mathbf{r}} \, \mathrm{d}\mathbf{r} = -\hat{f}(-\mathbf{k}). \tag{A4}$$

Similarly when f is an even function we have

$$\hat{f}(\mathbf{k}) = \int_{\mathbb{R}^d} f(\mathbf{r}) e^{-i\mathbf{k}\cdot\mathbf{r}} \, \mathrm{d}\mathbf{r} = \int_{\mathbb{R}^d} f(-\mathbf{r}) e^{i\mathbf{k}\cdot\mathbf{r}} \, \mathrm{d}\mathbf{r} = \int_{\mathbb{R}^d} f(\mathbf{r}) e^{i\mathbf{k}\cdot\mathbf{r}} \, \mathrm{d}\mathbf{r} = \hat{f}(-\mathbf{k}). \tag{A5}$$

□

For two or more component functions component wise. For example for a function $f : \mathbb{R}^d \times \mathbb{R}^d \to \mathbb{R}$ we define the Fourier and inverse Fourier transformations as

$$f(\mathbf{r}, \mathbf{r}') = \int_{\mathbb{R}^d} \int_{\mathbb{R}^d} f(\mathbf{k}, \mathbf{k}') e^{i\mathbf{k}\cdot\mathbf{r}} e^{i\mathbf{k}'\cdot\mathbf{r}'} \frac{\mathrm{d}\mathbf{k}}{(2\pi)^d} \frac{\mathrm{d}\mathbf{k}'}{(2\pi)^d} \quad \text{and} \quad f(\mathbf{k}, \mathbf{k}') = \int_{\mathbb{R}^d} \int_{\mathbb{R}^d} f(\mathbf{r}, \mathbf{r}') e^{-i\mathbf{k}\cdot\mathbf{r}} e^{-i\mathbf{k}'\cdot\mathbf{r}'} \, \mathrm{d}\mathbf{r} \, \mathrm{d}\mathbf{r}' \tag{A6}$$

These definitions are particularly important when we must deal with systems without translation invariance. Notice one can combine these new definitions with the above theorem to realize that if a function of multiple variables is odd or even in a particular variable then it will also be odd or even in the corresponding variable in Fourier space, independently of all other variables.

In translation invariant systems any (two point) observable, say, f can at most be a function of the difference between the two points, i.e. $f(\mathbf{r}, \mathbf{r}') = f(\mathbf{r} - \mathbf{r}')$. So we might ask ourselves how the Fourier transform then exhibits this symmetry. The answer is as comes from the above

$$f(\mathbf{r}, \mathbf{r}') = \int_{\mathbb{R}^d} \int_{\mathbb{R}^d} f(\mathbf{k}, \mathbf{k}') e^{i\mathbf{k}\cdot\mathbf{r}} e^{i\mathbf{k}'\cdot\mathbf{r}'} \frac{\mathrm{d}\mathbf{k}}{(2\pi)^d} \frac{\mathrm{d}\mathbf{k}'}{(2\pi)^d} = \int_{\mathbb{R}^d} \int_{\mathbb{R}^d} f(\mathbf{k}, \mathbf{k}') e^{i\mathbf{k}\cdot(\mathbf{r}-\mathbf{r}')} e^{i(\mathbf{k}+\mathbf{k}')\cdot\mathbf{r}'} \frac{\mathrm{d}\mathbf{k}}{(2\pi)^d} \frac{\mathrm{d}\mathbf{k}'}{(2\pi)^d}. \tag{A7}$$

However since we know f can only be a function of $\mathbf{r} - \mathbf{r}'$ we must require $\mathbf{k} + \mathbf{k} = 0$ inside the integral, i.e. $f(\mathbf{k}, \mathbf{k}') \propto \delta(\mathbf{k} + \mathbf{k}')$. Intgrating over $\mathbf{k}'$ we are left with

$$f(\mathbf{r} - \mathbf{r}') = \int_{\mathbb{R}^d} f(\mathbf{k}) e^{i\mathbf{k}\cdot(\mathbf{r}-\mathbf{r}')} \frac{\mathrm{d}\mathbf{k}}{(2\pi)^d}. \tag{A8}$$

B A Tool for Evaluating Green's Functions Exactly in Real Space

In the main text we evaluate Green's functions and particularly the integral over Green's function over all momenta. These integrals are particularly annoying to evaluate as they are fourth order polynomials in the denominator. We shall only consider ourselves with one dimensional wires (or systems that depend only on the magnitude of the momentum $|\mathbf{k}| = k$). For the interest of covering both the formalism of p- and s-wave superconductivity we shall include both such terms in a 4×4 model–although it does not matter as it in principle could be a 2×2 model. Do note that this is not motivated by a particular physical system (although such common phases should exist). We consider a constant singlet gap $\Delta_S(\mathbf{k}) = \Delta_s$ and triplet gap[8] $\Delta_T(\mathbf{k}) = \Delta_t k$

$$\mathcal{G}_0(x,x') = \frac{1}{V}\sum_k \mathcal{G}_0(k,i\omega_n)e^{ik(x-x')} = -\int_{-\infty}^{\infty} \frac{i\omega_n + \xi_k\tau_3 + \Delta_s\tau_2\sigma_2 + \Delta_t k\tau_1\sigma_0}{\omega_n^2 + \xi_k^2 + \Delta_s^2 + \Delta_t^2k^2} e^{ik(x-x')}\frac{\mathrm{d}k}{2\pi}. \tag{B1}$$

In the approximation limit where $\mu \gg \Delta$ we might have changed to an energy integral and assumed constant density of states. However we may instead find an exact solution to this integral by keeping to the momentum coordinates. To do this we need to make an assumption about the renormalized electron energies: we assume a priori that there is a constant shift in the energy spectrum which may be absorbed into the chemical potential, i.e. $\xi_k = \varepsilon_k - \mu$. The exact form of this can be verified through the self-consistent process of the 1BA. In general we assume ξ_k to be even and in practice we employ $\varepsilon_k = \frac{\hbar^2k^2}{2m}$ where $\hbar = 1$ and m is the effective mass of the quasi-particles.

The denominator of eq. (B1) is a second order polynomial in ε_k, with coefficients

$$P(\varepsilon_k) := a\varepsilon_k^2 - 2b\varepsilon_k + c \quad \text{where} \quad a = 1, \quad 2b = 2(\mu - m\Delta_t^2) \quad \text{and} \quad c = \omega_n^2 + \mu^2 + \Delta_s^2. \tag{B2}$$

The solutions to this polynomial, P, denominator are then

$$R_\pm = b \pm \sqrt{b^2 - c} = \mu - m\Delta_t^2 \pm \sqrt{m^2\Delta_t^4 - 2m\mu\Delta_t^2 - \omega_n^2 - \Delta_s^2}. \tag{B3}$$

There are two important measures then, namely whether the determinant $D := b^2 - c = m^2\Delta_t^4 - 2m\mu\Delta_t^2 - \omega_n^2 - \Delta_s^2$ is positive or negative and secondly the relation between the size of $\sqrt{D}$ compared to b. The square root above is without ambiguity as we can pick the principle square root and define R_+ to be the solution of $\sqrt{D}$ in the upper half plane, i.e. $\mathrm{Im}(R_+) > \mathrm{Im}(b) > \mathrm{Im}(R_-)$. However if $\mathrm{Im}(D) = 0$ we need not apply this complicated solution.

We shall of course be using a relevant contour to solve eq. (B1). A curve which does this generally consists of a straight line along the real axis and a semi-circle encompassing the upper complex plane. We integrate this curve in a positive oriented direction. The integral along the semi-circle in the upper plane clearly goes to zero as the radius of said semi-circle goes to infinity. There will, in some cases, be poles scattered on the real axis, and we shall accommodate these by making protrusion in the straight line curve. If these poles are simple, they will contribute 'half' a residue. If, however, they are of higher order the semi-circle protrusions will diverge, meaning we will be unable to determine the value of eq. (B1) in these cases.

Going from energy space ε to momentum space k introduces another problem of how one should choose the square roots of $R_\pm$. The ambiguity in choosing the square root can be resolved by introducing the two roots

$$S_\pm^1 = \sqrt{r_\pm}\left[\cos\left(\pm\frac{\theta}{2}\right) + i\sin\left(\pm\frac{\theta}{2}\right)\right] \quad \text{and} \quad S_\pm^2 = \sqrt{r_\pm}\left[\cos\left(\pm\frac{\theta}{2}+\pi\right) + i\sin\left(\pm\frac{\theta}{2}+\pi\right)\right], \tag{B4}$$

such that $(S_\pm^1)^2 = (S_\pm^2)^2 = 2mR_\pm$, where $r_\pm = |R_\pm|/\sqrt{2m}$. Note that we always have $S_\pm^1 = -S_\pm^2$. The roots $S_\pm^{1(2)}$ are the poles of the integrand in k-space. Bellow we consider each of the manifold cases of where the poles can be located and the effect of how we must change the choice of contour. The final ambiguity is how to chose the angles θ. We pick a branch cut for the $\sqrt{-}$-function depending on the location of the roots $S_\pm^{1(2)}$, see Figure 11 for reference.

The integral of eq. (B1) then becomes

$$\begin{aligned}\mathcal{G}_0(x,x') &= -\int_{-\infty}^{\infty} \frac{i\tilde{\omega}_n + (\frac{k^2}{2m} - \tilde{\mu})\tau_3 + \Delta_s\tau_2\sigma_2 + \Delta_t k\tau_1\sigma_0}{(k-S_+^1)(k-S_-^1)(k-S_+^2)(k-S_-^2)} e^{ik(x-x')}\frac{\mathrm{d}k}{2\pi} \\ &= -\int_{-\infty}^{\infty} \frac{[i\tilde{\omega}_n + (\frac{k^2}{2m} - \tilde{\mu})\tau_3 + \Delta_s\tau_2\sigma_2]\cos(k(x-x')) + i\Delta_t k\sin(k(x-x'))\tau_1\sigma_0}{(k-S_+^1)(k-S_-^1)(k-S_+^2)(k-S_-^2)}\frac{\mathrm{d}k}{2\pi}.\end{aligned} \tag{B5}$$

[8] The important point here is that the 'triplet' pairing is odd in k.

We calculate each of the residual of each first order pole separately, applicable when $D \neq 0$

$$\mathrm{Res}(S_+^1) = \frac{[i\omega_n + (R_+ - \mu)\tau_3 + \Delta_s\tau_2\sigma_2]\cos\big(S_+^1(x-x')\big) + i\Delta_t S_+^1 \sin\big(S_+^1(x-x')\big)\tau_1\sigma_0}{4mS_+^1(R_+ - R_-)}, \tag{B6a}$$

$$\mathrm{Res}(S_+^2) = -\frac{[i\omega_n + (R_+ - \mu)\tau_3 + \Delta_s\tau_2\sigma_2]\cos\big(S_+^1(x-x')\big) + i\Delta_t S_+^1 \sin\big(S_+^1(x-x')\big)\tau_1\sigma_0}{4mS_+^1(R_+ - R_-)}, \tag{B6b}$$

$$\mathrm{Res}(S_-^1) = -\frac{[i\omega_n + (R_- - \mu)\tau_3 + \Delta_s\tau_2\sigma_2]\cos\big(S_-^1(x-x')\big) + i\Delta_t S_-^1 \sin\big(S_-^1(x-x')\big)\tau_1\sigma_0}{4mS_-^1(R_+ - R_-)}, \tag{B6c}$$

$$\mathrm{Res}(S_-^2) = \frac{[i\omega_n + (R_- - \mu)\tau_3 + \Delta_s\tau_2\sigma_2]\cos\big(S_-^1(x-x')\big) + i\Delta_t S_-^1 \sin\big(S_-^1(x-x')\big)\tau_1\sigma_0}{4mS_-^1(R_+ - R_-)}. \tag{B6d}$$

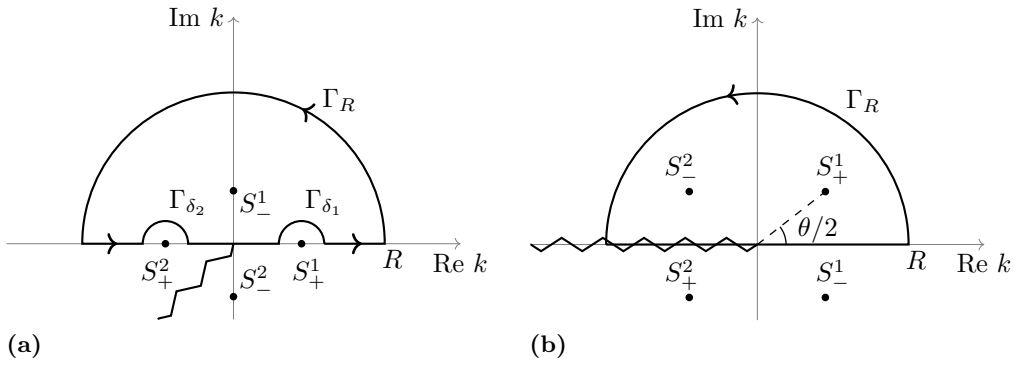

Figure 11: A typical contour of choice for integrating the Green's function. The rightmost figure represents a generic case where $D < 0$.

Let $\theta_\pm$ be the angle of the respective roots $R_\pm$. Depending on where in the complex plane these roots are determines which of the $S_\pm^{1(2)}$ should be counted in a contour integral. The two relevant parameters are $\mathrm{Im}(b)$ and $\mathrm{Im}(\sqrt{D})$. We may distinguish strict inequalities differentiating the phases depending on $x - x'$. If $x - x' > 0$ the exponential $e^{ik(x-x')}$ diverges when $\mathrm{Im}(k) \to -\infty$, so we have to pick a contour in the upper plane. Similarly when $x - x' < 0$ we must pick a contour in the lower plane. When $x - x' = 0$ we do not care and may pick the upper half-plane. When $x - x' > 0$ we may furcate the integral into the following cases of which poles should be counted in the residual sum:

(1) If $\mathrm{Im}(b) > \mathrm{Im}(\sqrt{D})$ and $\mathrm{Im}(b) > 0$ we count S_+^1 and S_-^1.

(2) If $\mathrm{Im}(\sqrt{D}) > \mathrm{Im}(b)$ and $\mathrm{Im}(\sqrt{D}) > 0$ we count S_+^1 and S_-^2.

(3) If $0 > \mathrm{Im}(\sqrt{D}) > \mathrm{Im}(b)$ we count S_+^2 and S_-^1.

(4) If $0 > \mathrm{Im}(b) > \mathrm{Im}(\sqrt{D})$ we count S_+^2 and S_-^2.

(5) If $\mathrm{Im}(b) = 0$ and $\mathrm{Im}(\sqrt{D}) \neq 0$ we count S_+^1 and S_-^2.

(6) If $\mathrm{Im}(b) > 0$ and $\mathrm{Im}(\sqrt{D}) = 0$ we count S_+^1 and S_-^1.

(7) If $\mathrm{Im}(b) < 0$ and $\mathrm{Im}(\sqrt{D}) = 0$ we count S_+^2 and S_-^2.

(8) If $\mathrm{Im}(b) = \mathrm{Im}(\sqrt{D}) = 0$:

a if $b < \sqrt{D}$ then we count only S_-^1, as both S_+^1 and S_+^2, which are on the real axis, cancel eachother.

b if $\sqrt{D} < -b$ then we count both S_+^1 and S_-^1.

Note that when $x - x' < 0$ we count the other poles effectively interchanging $S_\pm^1$ for $S_\pm^2$ and visa versa.

We see the transition between either 1. and 4. or 2. and 3 gives a sign change in the Green's function. so we might realistically only need to check if we are in 1. or 2.

Lets translate the conditions of the relation between $\mathrm{Im}(b)$ and $\mathrm{Im}(\sqrt{D})$ into inequalities for D, c and b. The translation for $\mathrm{Im}(b) = \mathrm{Im}(\tilde{\mu})$ is trivial. There is a closed expression for $\sqrt{D}$ namely if we write $D = x + iy$ where $x = \mathrm{Re}(D)$ and $y = \mathrm{Im}(D)$ we have

$$\sqrt{D} = \sqrt{x+iy} = \frac{1}{\sqrt{2}}\left(\sqrt{|D|+x} \pm i\sqrt{|D|-x}\right) = \frac{1}{\sqrt{2}}\left(\sqrt{|D|+x} + i\mathrm{sgn}(y)\sqrt{|D|-x}\right). \tag{B7}$$

The normal ambiguity of the square root may be absorbed into the definition of $R_\pm$. From this we find the exact condition that we should have $\mathrm{Im}(\sqrt{D}) \lessgtr \mathrm{Im}(b) \iff \mathrm{sgn}(\mathrm{Im}(D))\sqrt{|D| - \mathrm{Re}(D)} \lessgtr \mathrm{Im}(\tilde{\mu})$.

When we count S^1_+ and S^1_- we get

$$\mathcal{G}_0(x,x',i\omega_n) = -i\Bigg[\frac{[i\omega_n + (R_+ - \mu)\tau_3 + \Delta_s\tau_2\sigma_2]\cos\big(S^1_+(x-x')\big) + i\Delta_t S^1_+ \sin\big(S^1_+(x-x')\big)\tau_1\sigma_0}{4mS^1_+(R_+ - R_-)} \tag{B8}$$

$$- \frac{[i\omega_n + (R_- - \mu)\tau_3 + \Delta_s\tau_2\sigma_2]\cos\big(S^1_-(x-x')\big) + i\Delta_t S^1_- \sin\big(S^1_-(x-x')\big)\tau_1\sigma_0}{4mS^1_-(R_+ - R_-)}\Bigg] \tag{B9}$$

$$\mathcal{G}_0(x,x',i\omega_n) = -f_n\left[(i\omega_n + \Delta_s\tau_2\sigma_2)h_n(x-x') + g_n(x-x')\tau_3 + \Delta_t j_n(x-x')\tau_1\sigma_0\right], \tag{B10}$$

where the functions f, g, h and j are defined as follows

$$f_n := \frac{i}{8mS^1_+S^1_-\sqrt{D}}, \tag{B11a}$$

$$g_n(x-x') := (R_+ - \mu)S^1_-\cos\big(S^1_+(x-x')\big) - (R_- - \mu)S^1_+\cos\big(S^1_-(x-x')\big), \tag{B11b}$$

$$h_n(x-x') := S^1_-\cos\big(S^1_+(x-x')\big) - S^1_+\cos\big(S^1_-(x-x')\big), \tag{B11c}$$

$$j_n(x-x') := iS^1_+S^1_-[\sin\big(S^1_+(x-x')\big) - \sin\big(S^1_-(x-x')\big)]. \tag{B11d}$$

When we count S^1_+ and S^2_- we get

$$\mathcal{G}_0(x,x',i\omega_n) = -i\Bigg[\frac{[i\omega_n + (R_+ - \mu)\tau_3 + \Delta_s\tau_2\sigma_2]\cos\big(S^1_+(x-x')\big) + i\Delta_t S^1_+ \sin\big(S^1_+(x-x')\big)\tau_1\sigma_0}{4mS^1_+(R_+ - R_-)} \tag{B12}$$

$$+ \frac{[i\omega_n + (R_- - \mu)\tau_3 + \Delta_s\tau_2\sigma_2]\cos\big(S^1_-(x-x')\big) + i\Delta_t S^1_- \sin\big(S^1_-(x-x')\big)\tau_1\sigma_0}{4mS^1_-(R_+ - R_-)}\Bigg]. \tag{B13}$$

In this case the functions f, g, h and j are defined as follows

$$f_n := \frac{i}{8mS^1_+S^1_-\sqrt{D}}, \tag{B14a}$$

$$g_n(x-x') := (R_+ - \mu)S^1_-\cos\big(S^1_+(x-x')\big) + (R_- - \mu)S^1_+\cos\big(S^1_-(x-x')\big), \tag{B14b}$$

$$h_n(x-x') := S^1_-\cos\big(S^1_+(x-x')\big) + S^1_+\cos\big(S^1_-(x-x')\big), \tag{B14c}$$

$$j_n(x-x') := iS^1_+S^1_-[\sin\big(S^1_+(x-x')\big) + \sin\big(S^1_-(x-x')\big)]. \tag{B14d}$$

Notice in both cases if $x - x' = 0$ then $h = S^1_- \pm S^1_+$ (depending on the specific case) and $j = 0$. Furthermore when the sign of $x - x'$ changes and we have to interchange $S^1_\pm$ and $S^2_\pm$ both f and j stay the same while g and h change sign.

In the case where $b < \sqrt{D}$ and only S^1_- is counted

$$\mathcal{G}_0(x,x',i\omega_n) = i\frac{[i\omega_n + (R_- - \mu)\tau_3 + \Delta_s\tau_2\sigma_2]\cos\big(S^1_-(x-x')\big) + i\Delta_t S^1_- \sin\big(S^1_-(x-x')\big)\tau_1\sigma_0}{4mS^1_-(R_+ - R_-)} \tag{B15}$$

So the functions f, g, h and j simplify significantly compared to the other cases

$$f_n := \frac{i}{8mS^1_-\sqrt{D}}, \tag{B16a}$$

$$g_n(x-x') := (R_- - \mu)\cos\big(S^1_-(x-x')\big), \tag{B16b}$$

$$h_n(x-x') := \cos\big(S^1_-(x-x')\big), \tag{B16c}$$

$$j_n(x-x') := iS^1_-\sin\big(S^1_-(x-x')\big). \tag{B16d}$$

Particularly when $x - x' = 0$ then $g = (R_- - \mu)$, $h = 1$ and $j = 0$.

Do note in the three cases we have just outlined the functions g and h are even functions of $x - x'$ while j is the only odd function.

B.1 The DOS and Non-Local SC1BA for two state systems

Lets now apply the theory we have just developed for finding the bare Green's function $\mathcal{G}_0$ to finding the self-energy as described in SC1BA. The self-consistent equation in the Born approximation is

$$\mathcal{G} = \mathcal{G}_0 - \Sigma. \tag{B17}$$

As we found in the last previous chapter the bare Green's Function can be written in term of the functions f, g, h, j which are dependent on the Matsubara frequency $i\omega_n$, the chemical potential μ and the gap functions Δ_s or Δ_t. Remember we only really care about the cases when either we're modeling a s-wave superconductor, i.e. $\Delta_t = 0$, or a p-wave superconductor, i.e. $\Delta_s = 0$. The bare Green's Function of our toy model is

$$\mathcal{G}_0(x, x') = -f_n \left[(i\omega_n + \Delta_s \tau_2\sigma_2) h_n(x - x') + g_n(x - x')\tau_3 + \Delta_t j_n(x - x')\tau_1\sigma_0 \right]. \tag{B18}$$

We can use a similar parametrization for the full Green's Function $\mathcal{G}$, we shall use $\sim$ above the parameters to denote they are renormalized though the SC1BA,

$$\mathcal{G}^{-1}(k) = i\tilde{\omega}_n - \tilde{\xi}_k\tau_3 - \tilde{\Delta}_S(k)\tau_2\sigma_2 - \tilde{\Delta}_T(k)\tau_1\sigma_0. \tag{B19}$$

Using similar singlet and triplet pairing functions as above, i.e. $\tilde{\Delta}_S(\mathbf{k}) = \tilde{\Delta}_s$ and $\tilde{\Delta}_T(\mathbf{k}) = \tilde{\Delta}_t k$, the self-consistent equation reads

$$\begin{aligned} \Sigma &= (i\omega_n - i\tilde{\omega}_n) - (\xi_k - \tilde{\xi}_k)\tau_3 - (\Delta_s - \tilde{\Delta}_s)\tau_2\sigma_2 - (\Delta_t k - \tilde{\Delta}_t k)\tau_1\sigma_0 \\ &= -\tilde{f}_n \frac{1}{\tau_i} \left[(i\tilde{\omega}_n - \tilde{\Delta}_s\tau_2\sigma_2)\tilde{h}_n + \tilde{g}_n\tau_3 \right] - \tilde{f}_n \frac{1}{\tau_\beta} \left[(i\tilde{\omega}_n + \tilde{\Delta}_s\tau_2\sigma_2)\tilde{h}_n + \tilde{g}_n\tau_3 \right], \end{aligned} \tag{B20}$$

the tilde on the functions, e.g. $\tilde{f}$, signifies they are evaluated in the renormalized parameters such as $i\tilde{\omega}_n$ and $\tilde{\mu}$. Furthermore we omit the argument $x - x' = 0$ here as we are only interested in the global density of states for now. Define the familiar τ_i^{-1} and τ_β^{-1} as

$$\tau_i^{-1} := N_i |U_1|^2 \quad \text{and} \quad \tau_\beta^{-1} := S(S+1) N_\beta |U_2|^2. \tag{B21}$$

Here we have calculated the impurity potentials through the following argument

$$|v_{k-k'}|^2 = |V|^2 \sum_{ij} e^{-(k-k')(R_i - R_j)} = |V|^2 \sum_{i=j} e^{-(k-k')(R_i - R_j)} + |V|^2 \sum_{i \neq j} e^{-(k-k')(R_i - R_j)} \tag{B22}$$

Clearly the first sum gives gives N_i. The second sum can be expressed in terms of cosines as all the i sin terms cancel under the exchange of i and j. Then for any specific i the of the j's will roughly cancel if we assume the impurities to be uniformly distributed. The same result can be achieved using the Dirichlet kernel. Similarly for the spin dependent potential

$$|w_{ik-k'}|^2 = |W|^2 \sum_{\beta\beta'} S^i_\beta S^j_{\beta'} e^{-(k-k')(R_\beta - R_{\beta'})} = |W|^2 \sum_{\beta=\beta'} S^i_\beta S^j_{\beta'} e^{-(k-k')(R_\beta - R_{\beta'})} + |W|^2 \sum_{\beta\neq\beta'} S^i_\beta S^j_{\beta'} e^{-(k-k')(R_\beta - R_{\beta'})} \tag{B23}$$

where under the spin average $\langle S^i_\beta S^j_\beta \rangle = \frac{1}{3} S(S+1)\delta_{ij}$.

The self-consistent equation can be broken down component wise to obtain the following set of equations, one for each system parameter

$$i\tilde{\omega}_n = i\omega_n + \tilde{f}\tilde{h} \left[\frac{1}{\tau_i} + \frac{1}{\tau_\beta} \right] i\tilde{\omega}_n, \quad \tilde{\mu} = \mu + \tilde{f}\tilde{g} \left[\frac{1}{\tau_i} + \frac{1}{\tau_\beta} \right], \quad \tilde{\Delta}_s = \Delta_s + \tilde{f}\tilde{h} \left[\frac{1}{\tau_i} - \frac{1}{\tau_\beta} \right] \tilde{\Delta}_s \quad \text{and} \quad \tilde{\Delta}_t = \Delta_t. \tag{B24}$$

The density of states is then

$$A(i\omega_n) = \operatorname{Im} \left[\tilde{f}(i\tilde{\omega}_n \tilde{h} + \tilde{g}\tau_3) \right] \tag{B25}$$

When picking an energy scale (frequency) for the density of states (or just the Green's function) it is commonplace to normalize the parameter such that the DOS has singularities when the parameter is 1. For the usual BCS DOS $\approx \omega/\sqrt{\Delta^2 - \omega^2}$ one uses ω/Δ as a plotting parameter. In our formalism we have four singularities (in ω), not two, but in the limit $\mu \to \infty$ we may focus our attention on the solutions of D:

$$0 \overset{!}{=} D = m^2\Delta_t^4 - 2m\mu\Delta_t^2 + \omega^2 - \Delta_s^2 \iff \omega = \pm\sqrt{\Delta_s^2 + 2m\mu\Delta_t^2 - m^2\Delta_t^4}. \tag{B26}$$

Notice in the case when $\Delta_t = 0$, i.e. a pure s-wave superconductor the singularity we obtain the same scale as from BCS theory. However for a pure p-wave superconductor we may rescale ω by a factor $\sqrt{2m\mu\Delta_t^2 - m^2\Delta_t^4}^{-1}$.

The other singularities along the diagonal of $\mathcal{G}_0$, come from f and are either S^1_+ or S^1_- or just S^1_-. $S^1_\pm$ are zero exactly when $R_\pm$ are, so solving

$$R_\pm = (\mu - m\Delta_t^2)^2 \pm \sqrt{(\mu - m\Delta_t^2)^2 + \omega^2 - \Delta_s^2 - \mu^2} = 0, \tag{B27}$$

for ω, gives solutions

$$\omega = \pm\sqrt{\Delta_s^2 + \mu^2}. \tag{B28}$$

These singularities are $O(\mu)$, however, and therefore quickly become irrelevant as μ becomes increasingly large. To be exact the function $\frac{1}{S^1_\pm}$ drops off as $\frac{1}{\sqrt{\omega}}$, i.e. $\frac{1}{S^1_\pm} = O(\omega^{-1/2})$, so for sufficiently large chemical potential we need not concern ourselves with this.

Often the density of the superconducting state is normalized against the normal state density of states at the Fermi level $d_n(0) = \sqrt{\frac{2m}{\mu}}$. However for our case the density of state in the normal state system will be dependent on the frequency and the chemical potential. Instead we can normalize by the normal state density of states without using the large μ approximation. In actuallity we simply devide by the Green's function found above in eq. (B10) setting the gap to zero. This will give us the normal state density of states which we write as follows

$$\mathcal{G}_N(x, x', i\omega_n) = -f_n|_{\Delta=0}\left[i\omega_n h_n|_{\Delta=0}(x - x') + g_n|_{\Delta=0}(x - x')\tau_3\right] \tag{B29}$$

The functions f_n still have the same regimes only we set Δ_s and Δ_t to zero, e.g. in the regieme

$$f_n := \frac{i}{8mS^1_+S^1_-\sqrt{D}}, \tag{B30a}$$

$$g_n(x - x') := (R_+ - \mu)S^1_- \cos\big(S^1_+(x - x')\big) + (R_- - \mu)S^1_+ \cos\big(S^1_-(x - x')\big), \tag{B30b}$$

$$h_n(x - x') := S^1_- \cos\big(S^1_+(x - x')\big) + S^1_+ \cos\big(S^1_-(x - x')\big), \tag{B30c}$$

$$j_n(x - x') := iS^1_+S^1_-[\sin\big(S^1_+(x - x')\big) + \sin\big(S^1_-(x - x')\big)], \tag{B30d}$$

the roots are simpler $S^1_\pm = \sqrt{\mu \pm \sqrt{-\omega_n^2}}$ and the variable D simplifies significantly to $D = \mu \pm \sqrt{-\omega_n^2}$.

At this point it should be of interest to the reader if these self-consistent equations from this 4×4 toy model really are isomorphic to those of the 2×2 low energy model, eq. (2.52), found in Section 2.3 with the impurities as in eq. (2.56). The impurity potentials used in the low energy model are

$$\mathcal{V}_{\text{eff}}(k) := v_k\sigma_3 \quad \text{and} \quad \mathcal{W}_{\text{eff}}(k) := -w_{2,k}\sigma_3 - \frac{uk}{B}w_{3,k}\sigma_0. \tag{B31}$$

Written out in full the self-energy in the SC1BA is

$$\Sigma(k) = \frac{1}{V}\sum_{k'} \mathcal{V}_{\text{eff}}(k - k')\mathcal{G}(k')\mathcal{V}_{\text{eff}}(k' - k) + \frac{1}{V}\sum_{k'} \mathcal{W}_{\text{eff}}(k - k')\mathcal{G}(k')\mathcal{W}_{\text{eff}}(k' - k) \tag{B32}$$

$$= \frac{1}{V}\sum_{k'} |v_{k-k'}|^2\mathcal{G}(-k', i\omega_n) \tag{B33}$$

$$+ \frac{1}{V}\sum_{k'} \left(w_{2,k-k'}\sigma_3 + \frac{u(k - k')}{B}w_{3,k-k'}\right)\mathcal{G}(k', i\omega_n)\left(w_{2,k'-k}\sigma_3 + \frac{u(k' - k)}{B}w_{3,k'-k}\right), \tag{B34}$$

where the impurity averaged Green's Function is picked to be

$$\mathcal{G}^{-1}(k, i\omega_n) = i\tilde{\omega}_n - \tilde{\xi}_k\sigma_3 - \tilde{\Delta}k\sigma_2. \tag{B35}$$

The first term, i.e. eq. (B33), is already of a similar structure as that to the 4×4 model. In the second term, expressions like

$$\frac{u(k - k')}{B}w_{3,k-k'}\mathcal{G}(k', i\omega_n)\frac{u(k' - k)}{B}w_{3,k'-k} \propto \frac{u^2k^2}{B^2}, \tag{B36}$$

are suppressed by the assumption $uk \ll B$ and can effectively be ignored[9]. Furthermore the cross terms

$$w_{2,k-k'}\sigma_3\mathcal{G}(k', i\omega_n)\frac{u(k' - k)}{B}w_{3,k'-k} + \frac{u(k - k')}{B}w_{3,k-k'}\mathcal{G}(k', i\omega_n)w_{2,k'-k}\sigma_3 \propto S_{2,\beta}S_{3,\beta'}, \tag{B37}$$

are identically zero after averaging over spins. Leaving only contribution from the term

$$w_{2,k-k'}\sigma_3\mathcal{G}(k', i\omega_n)w_{2,k'-k}\sigma_3 = |w_{2,k-k'}|^2\mathcal{G}(-k', i\omega_n). \tag{B38}$$

[9] Although this is formally untrue and the self-energy should always diverge we ignore the terms anyways

B.2 Interpreting Data and the s+p-wave Phase

The program solves the set of self-consistent equations, for each point in an interval of discretized frequency space and finds the density of states, and for each regime as defined above. The density of states defined in the program is a convex sum all regimes, of the truth value (1 or 0) of the regime times the specific density of states in that regime as found by the respective self-consistent equations.

A single impurity scan of two systems, one with $\Delta_t = 1$ and $\Delta_s = 1$ and the other with $\Delta_t = 1$ and $\Delta_s = 0$, leads me to the conclusion that $\tilde{\Delta}_t$ and $\tilde{\Delta}_s$ are linearly independent as the two system configurations produce the same density of states.

It seems for a pure p-wave SC the gap closes around $\tau_\beta^{-1} \approx 8m^2\Delta\mu$. While for the pure s-wave SC it is determined by $\tau_\beta^{-1} \approx \Delta\sqrt{8m^3\mu}$.

B.3 The position dependent DOS in 1BA

We wish to analyze the position dependent density of states of a system which is not necessarily translation invariant. To do this we take a step back an reflect on the general form of the Dyson equation for non interacting scattering events. The general equation reads

$$\mathcal{G}(a,b) = \mathcal{G}_0(a,b) + \int \mathcal{G}_0(a,c)V(c)\mathcal{G}(c,b)\,\mathrm{d}c\,. \tag{B39}$$

Here we use the index placeholder notation, i.e. a, b and c can be taken to mean, e.g., either mean real space or momentum index. One can use the recursive nature of this equation to define the self-energy in the first born approximation as

$$\Sigma(c,d) = V(c)\mathcal{G}_0(c,d)V(d) \tag{B40}$$

so that the first Born Green's function is

$$\mathcal{G}^{\mathrm{1BA}}(a,b) = \mathcal{G}_0(a,b) + \iint \mathcal{G}_0(a,c)V(c)\mathcal{G}_0(c,d)V(d)\mathcal{G}_0(d,b)\,\mathrm{d}c\,\mathrm{d}d \tag{B41}$$

In the present case of spinful and spinless impurity potentials in a 1D TS wire, we have with the above notation

$$\Sigma^{1BA}(x,x') = \mathcal{V}(x)\mathcal{G}_0(x,x')\mathcal{V}(x') + \mathcal{W}(x)\mathcal{G}_0(x,x')\mathcal{W}(x') \tag{B42}$$

In the self-consistent Born approximation we replace $\mathcal{G}$ with $\mathcal{G}$, giving

$$\Sigma^{SC1BA}(x,x') = \mathcal{V}(x)\mathcal{G}(x,x')\mathcal{V}(x') + \mathcal{W}(x)\mathcal{G}(x,x')\mathcal{W}(x') \tag{B43}$$

In the effective model we replace the potentials by the effective 2×2 potential interactions, i.e. $\mathcal{V} \to \mathcal{V}_{\mathrm{eff}}$ and $\mathcal{W} \to \mathcal{W}_{\mathrm{eff}}$.

C The Self-Consistency Condition and Origin of the Gap Function

Within BCS theory the interaction potential gives rise to the gap function and how this comes about is the topic of this section. Using a maximally [debate me] generalized potential with indices α and β indicating some discrete degrees of freedom, this can be spin or orbital index. The interaction potential is then

$$V = \sum_{\mathbf{k}\mathbf{k}',\alpha\beta} V^{\alpha\beta}_{\mathbf{k}\mathbf{k}'} \psi^\dagger_\alpha(\mathbf{k})\psi^\dagger_\beta(-\mathbf{k})\psi_\beta(-\mathbf{k}')\psi_\alpha(\mathbf{k}'). \tag{C1}$$

Where $(V^{\alpha\beta}_{\mathbf{k}\mathbf{k}'})^* = V^{\alpha\beta}_{\mathbf{k}'\mathbf{k}}$, since V is assumed hermitian, and additionally the following must be true from the Fock algebra $V^{\alpha\beta}_{\mathbf{k}\mathbf{k}'} = V^{\beta\alpha}_{-\mathbf{k}-\mathbf{k}'}$. Doing a Hartree-Fock mean field approximation in the pair creation and annihilation operators, we find

$$V^{\mathrm{MF}} = \sum_{\mathbf{k}\mathbf{k}',\alpha\beta} \Big[V^{\alpha\beta}_{\mathbf{k}\mathbf{k}'} \psi^\dagger_\alpha(\mathbf{k})\psi^\dagger_\beta(-\mathbf{k}) \left\langle \psi_\beta(-\mathbf{k}')\psi_\alpha(\mathbf{k}') \right\rangle + V^{\alpha\beta}_{\mathbf{k}\mathbf{k}'} \left\langle \psi^\dagger_\alpha(\mathbf{k})\psi^\dagger_\beta(-\mathbf{k}) \right\rangle \psi_\beta(-\mathbf{k}')\psi_\alpha(\mathbf{k}') \tag{C2}$$

$$+ V^{\alpha\beta}_{\mathbf{k}\mathbf{k}'} \left\langle \psi^\dagger_\alpha(\mathbf{k})\psi^\dagger_\beta(-\mathbf{k}) \right\rangle \left\langle \psi_\beta(-\mathbf{k}')\psi_\alpha(\mathbf{k}') \right\rangle \Big]. \tag{C3}$$

The last term is just a constant term which can be absorbed into the chemical potential of a given model. Explicitly defining the pairing $\Delta_{\alpha\beta}(\mathbf{k}) := \sum_{\mathbf{k}'} V^{\alpha\beta}_{\mathbf{k}\mathbf{k}'} \left\langle \psi_\beta(-\mathbf{k}')\psi_\alpha(\mathbf{k}') \right\rangle$, we obtain the familiar (almost) BCS Hamiltonian

$$V^{\mathrm{MF}} = \sum_{\mathbf{k},\alpha\beta} \Big[\Delta_{\alpha\beta}(\mathbf{k})\psi^\dagger_\alpha(\mathbf{k})\psi^\dagger_\beta(-\mathbf{k}) + \Delta^*_{\alpha\beta}(\mathbf{k})\psi_\beta(-\mathbf{k})\psi_\alpha(\mathbf{k}) \Big]. \tag{C4}$$

Notice the symmetry the gap function inherits from the potential interaction is

$$\Delta_{\alpha\beta}(\mathbf{k}) = -\sum_{\mathbf{k}'} V^{\beta\alpha}_{-\mathbf{k}-\mathbf{k}'} \left\langle \psi_\alpha(\mathbf{k}')\psi_\beta(-\mathbf{k}') \right\rangle = -\sum_{\mathbf{k}'} V^{\beta\alpha}_{-\mathbf{k}\mathbf{k}'} \left\langle \psi_\alpha(-\mathbf{k}')\psi_\beta(\mathbf{k}') \right\rangle = -\Delta_{\beta\alpha}(-\mathbf{k}). \tag{C5}$$

The most common use of the above calculations would be when the indices α, β represent spin degrees of freedom (isomorphic to two orbit models). Written out the mean field potential becomes

$$V^{\mathrm{MF}} = \sum_{\mathbf{k}} \Big[\Delta_{\uparrow\uparrow}(\mathbf{k})\psi^\dagger_\uparrow(\mathbf{k})\psi^\dagger_\uparrow(-\mathbf{k}) + \Delta^*_{\uparrow\uparrow}(\mathbf{k})\psi_\uparrow(-\mathbf{k})\psi_\uparrow(\mathbf{k}) + \Delta_{\downarrow\downarrow}(\mathbf{k})\psi^\dagger_\downarrow(\mathbf{k})\psi^\dagger_\downarrow(-\mathbf{k}) + \Delta^*_{\downarrow\downarrow}(\mathbf{k})\psi_\downarrow(-\mathbf{k})\psi_\downarrow(\mathbf{k})$$

$$+ \Delta_{\uparrow\downarrow}(\mathbf{k})\psi^\dagger_\uparrow(\mathbf{k})\psi^\dagger_\downarrow(-\mathbf{k}) + \Delta^*_{\uparrow\downarrow}(\mathbf{k})\psi_\downarrow(-\mathbf{k})\psi_\uparrow(\mathbf{k}) + \Delta_{\downarrow\uparrow}(\mathbf{k})\psi^\dagger_\downarrow(\mathbf{k})\psi^\dagger_\uparrow(-\mathbf{k}) + \Delta^*_{\downarrow\uparrow}(\mathbf{k})\psi_\uparrow(-\mathbf{k})\psi_\downarrow(\mathbf{k}) \Big]. \tag{C6}$$

If we assume the pairing potential to be the same for in up and down triplets, by using the Fermion algebra and the symmetry of the gap we find

$$V^{\mathrm{MF}} = \sum_{\mathbf{k}\sigma} \Big[\Delta_T(\mathbf{k})\psi^\dagger_\sigma(\mathbf{k})\psi^\dagger_\sigma(-\mathbf{k}) + h.c. \Big] + \sum_{\mathbf{k}} \Big[\Delta_S(\mathbf{k})\psi^\dagger_\uparrow(\mathbf{k})\psi^\dagger_\downarrow(-\mathbf{k}) + h.c. \Big], \tag{C7}$$

where

$$\Delta_S(\mathbf{k}) := 2\Delta_{\uparrow\downarrow}(\mathbf{k}) = 2\sum_{\mathbf{k}'} V^{\uparrow\downarrow}_{\mathbf{k}\mathbf{k}'} \left\langle \psi_\downarrow(-\mathbf{k}')\psi_\uparrow(\mathbf{k}') \right\rangle \quad \text{and} \quad \Delta_T(\mathbf{k}) := \Delta_{\uparrow\uparrow}(\mathbf{k}) = \sum_{\mathbf{k}'} V^{\uparrow\uparrow}_{\mathbf{k}\mathbf{k}'} \left\langle \psi_\uparrow(-\mathbf{k}')\psi_\uparrow(\mathbf{k}') \right\rangle. \tag{C8}$$

Clearly $\Delta_T(\mathbf{k}) = -\Delta_T(-\mathbf{k})$, which may be seen directly from the definition and eq. (C5).

D A Useful Approximation for the Non-Local Density of States

D.1 In the Normal State

In the normal state the Green's function is rather simple

$$\mathcal{G}_0(\mathbf{k}, i\omega_n) = \frac{i\omega_n + \xi_{\mathbf{k}}\tau_3}{\omega_n^2 + \xi_{\mathbf{k}}^2}. \tag{D1}$$

In either the particle or hole block this corresponds to

$$G_0^{p/h}(\mathbf{k}, i\omega_n) = \frac{1}{i\omega \mp \xi_{\mathbf{k}}}, \tag{D2}$$

where the minus corresponds to the particle and the plus corresponds to the hole Green's functions. The corresponding spectral function is easily found

$$A_0^{p/h}(\mathbf{k}, i\omega_n) = -2\mathrm{Im}G_0^{p/h,R}(\mathbf{k}, \omega) = -2\mathrm{Im}\left[\mp i\pi\delta(\omega - \xi_{\mathbf{k}}) + \mathcal{P}\left(\frac{1}{\omega - \xi_{\mathbf{k}}}\right)\right]. \tag{D3}$$

D.2 In the Superconducting State

We wish to find a general expression for the density of states from the GF formalism, without making any assumptions on the dependence of Δ on frequency ω. The (retarded) superconducting Green's Function reads

$$G(\mathbf{k}, \omega + i\eta) = \frac{\omega + i\eta + \xi_{\mathbf{k}}\tau_3 + \Delta_0\tau_1}{(\omega + i\eta)^2 - \xi_{\mathbf{k}}^2 - \Delta_0^2} = \frac{\omega + i\eta + \xi_{\mathbf{k}}\tau_3 + \Delta_0\tau_1}{(\omega + i\eta)^2 - E_{\mathbf{k}}^2} \quad \text{where} \quad E_{\mathbf{k}} := \sqrt{\xi_{\mathbf{k}}^2 + \Delta_0^2}. \tag{D4}$$

Where $\xi_{\mathbf{k}}$ is the quasi-particle spectrum Δ_0 is the superconducting gap, assumed constant in $\mathbf{k}$. The corresponding density of states is

$$\begin{aligned} d_s(\omega) = \frac{1}{2\pi V}\sum_{\mathbf{k},\sigma} A_\sigma(\mathbf{k}, \omega) &= -\lim_{\eta\to 0}\frac{1}{\pi V}\sum_{\mathbf{k}\sigma}\mathrm{Im}[G_{\sigma\sigma}(\mathbf{k}, \omega + i\eta)] \\ &= -\lim_{\eta\to 0}\frac{1}{\pi V}\sum_{\mathbf{k}\sigma}\mathrm{Im}\left\{\left[\frac{1}{\omega + i\eta - E_{\mathbf{k}}} - \frac{1}{\omega + i\eta + E_{\mathbf{k}}}\right]\frac{\omega + i\eta + \xi_{\mathbf{k}}}{2E_{\mathbf{k}}}\right\}. \end{aligned} \tag{D5}$$

The $i\eta$ term goes to zero in the limit case and can be ignored. The other terms reduce from the Sokhotski–Plemelj theorem. A standard method for evaluating these is to extend $\min(\xi) \to \infty$ which is exactly $\mu \to -\infty$ and then shifting to an energy integral. So that

$$\begin{aligned} d_s(\omega) &= -\frac{1}{\pi V}\mathrm{Im}\sum_{\mathbf{k}\sigma}\left[-\pi i\delta(\omega - E_{\mathbf{k}}) + \mathcal{P}\frac{1}{\omega - E_{\mathbf{k}}} + \pi i\delta(\omega + E_{\mathbf{k}}) - \mathcal{P}\frac{1}{\omega + E_{\mathbf{k}}}\right]\frac{\omega + \xi_{\mathbf{k}}}{2E_{\mathbf{k}}} \\ &= \frac{d_0}{2}\mathrm{Re}\int_{-\infty}^{\infty}[\delta(\omega - E) - \delta(\omega + E)]\frac{\omega + \xi}{E}\,\mathrm{d}\xi \\ &= \frac{d_0}{2}\mathrm{Re}\int_{-\infty}^{\infty}\left(1 + \frac{\xi}{E}\right)\delta(\omega - E) + \left(1 - \frac{\xi}{E}\right)\delta(\omega + E)\,\mathrm{d}\xi \end{aligned} \tag{D6}$$

where d_0 is the normal state density of states at the Fermi level. Since ξ/E is odd in ξ those two terms drop out leaving us with

$$\frac{d_s(\omega)}{d_0} = \frac{1}{2}\mathrm{Re}\int_{-\infty}^{\infty}\delta(\omega - E) + \delta(\omega + E)\,\mathrm{d}\xi\,. \tag{D7}$$

The roots for both functions $f_\pm := \omega \pm E$, w.r.t. ξ, are $\xi_\pm = \pm\sqrt{\omega^2 - \Delta_0^2}$ and their derivatives are $f'_\pm = \pm\frac{\xi}{\sqrt{\xi^2 + \Delta_0^2}}$. However we wish to only count the real solutions of ξ so for $\delta(\omega - E)$ we must have $\omega > \Delta_0$ and for

$\delta(\omega + E)$ we must have $\omega > -\Delta_0$. In effect the integral can be rewritten as

$$\begin{aligned}
\frac{N(\omega)}{N_0} &= \frac{1}{2}\mathrm{Re}\int_{-\infty}^{\infty} \delta(\omega - E)\theta(\omega - \Delta_0) + \delta(\omega + E)\theta(-\omega - \Delta_0)\,\mathrm{d}\xi \\
&= \frac{1}{2}\mathrm{Re}\sum_{\pm}\left[\frac{1}{|f'_-(\xi_\pm)|}\theta(\omega - \Delta_0) + \frac{1}{|f'_+(\xi_\pm)|}\theta(-\omega - \Delta_0)\right] \\
&= \mathrm{Re}\left[\frac{|\omega|}{\sqrt{\omega^2 - \Delta_0^2}}\theta(\omega - \Delta_0) + \frac{|\omega|}{\sqrt{\omega^2 - \Delta^2}}\theta(-\omega - \Delta_0)\right] \\
&= \mathrm{Re}\frac{|\omega|}{\sqrt{\omega^2 - \Delta_0^2}}\theta(|\omega| - \Delta_0)
\end{aligned} \tag{D8}$$

Notice if for some reason there could be energy states with $|\omega| < \Delta_0$ such would be the case if Δ_0 was dependent on ω and simply taking the real part would ensure the density of states is zero within the gap. An alternate from often seen in the literature reads

$$\frac{N(\omega)}{N_0} = \mathrm{Re}\frac{|\omega|}{\sqrt{\omega^2 - \Delta_0^2}} \tag{D9}$$